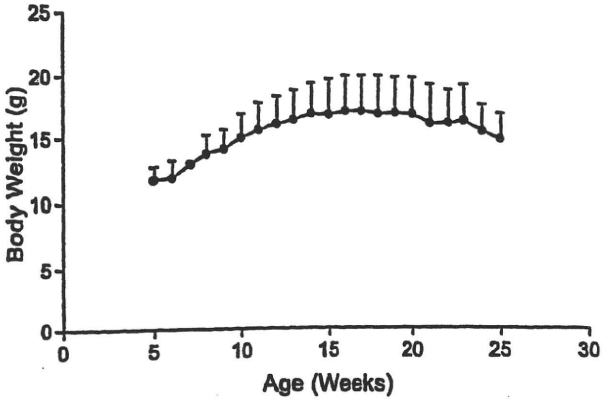

図6　PXBマウスの体重推移

10週齢を経過すると，15g以上の体重を維持する。

4. PXBマウスの実験への利用

PXBマウスには，野生型のマウスに準じて多様な実験処置を施すことが可能である。当所で実施している試験操作の中から，被験物質の投与と生体試料の採取方法について具体例を挙げる。被験物質の投与については，投与経路として経口，皮下，腹腔内，静脈内，筋肉内など一般的な経路の他に，麻酔下動物の静脈内への持続的な投与や肝臓への直接投与などの特殊な経路も選択できる。一般的な投与経路については，1日あたり複数回(3回を上限として設定)の投与や，反復投与(2週間の実施が最も多い)も実施可能である。採取可能な生体試料の項目は，経時／連続採取可能なものとして，血液，胆汁，尿および糞，解剖時には各種組織および器官の採取が可能である。このうち，血液は10μL/g BW/1 week，胆汁は5μL/h，尿は1.0 mL/24 h，糞は1.5 g/24 hが採取量の目安となっている。これらの操作は，一般状態観察および体重測定によって個体の健康状態を把握しながら実施されている。また，肝炎ウイルスなど感染性微生物を感染させたPXBマウスについては，作業者への感染リスクが大きくならないことを事前に判断した上で各種の処置や生体試料の採取を実施している。なお，当所では，これらPXBマウスの利用方法の詳細について，所内に設けた倫理委員会で審査・承認を行っている。

以降には，PXBマウスの実用例の一部として，特に医薬品開発に関連する薬物代謝，肝毒性および肝炎ウイルスについての研究成果を紹介する。

薬物代謝は，医薬品開発の過程においてヒトでの薬効と毒性を正しく理解するために重要な研究分野である。この分野においてPXBマウスに期待される点は，PXBマウス肝臓内のヒト肝細胞がヒト生体と同様の薬物代謝機能を有していることである。

現在までに当所において生産されたPXBマウスのうち，3ロットの異なるドナー肝細胞を用いて生産されたPXBマウスの肝臓について，DNAアレイ(Affymetrix GeneChip® Human Genome U133 plus 2.0 Array，38,500遺伝子を解析可能)を用いた遺伝子発現解析を実施したところ，PXBマウス肝臓内のヒト肝細胞では，当該アレイに搭載されたヒト遺伝子のうち，70％にあたる遺伝子の発現が確認され，このうち98％に相当する遺伝子については3ロット間の発現量に大きな差(2倍未満または1/2より大きい)は認められなかった。

ヒト肝細胞に発現している多数の分子のうち，薬物代謝酵素に注目すると，第I相反応を担うチトクロームP450(CYP)に含まれる主要な分子種であるCYP1A1，1A2，2A6，3A4，3A5，2C9，2C8，2C19，および2D6の発現が確認されており[3),11)-13)]また，アルデヒドオキシダーゼについても発現が確認されている[14)]。このうち，CYP2A6，3A4，2C8，2C9，2C19および2D6については，PXBマウスの置換率上昇に伴って酵素活性が上昇を示すことが報告されており[11)]，また，CYP2A6，2C19および2D6については，ドナーの遺伝子多型由来と考えられる酵素活性の差が確認されている[11),15)]。第II相反応を担う酵素については，グルクロン酸抱合酵素(UGT)，硫酸抱合酵素(SULT，CSTおよびTPST)，アセチル抱合酵素(NAT)，グルタチ

オン抱合酵素(GSTおよびMGST)，メチル抱合酵素(COMT，PNMT，TPMT，GAMT，PEMTおよびASMT)に含まれる主要な分子種の発現が確認されている[12),16)]。これらの酵素に含まれる分子種のうち，UGT2B7，SULT1A1，SULT1E1およびNAT2については，PXBマウスの置換率上昇に伴って酵素活性が高値を示すことも報告されており[16)]，NAT2の酵素活性についてはドナー肝細胞の遺伝子多型に由来すると考えられるドナー間差が確認されている[16)]。化学物質を肝細胞内外に輸送する機能を持つトランスポーターについても，ABCトランスポーター(ABCA)，Solute carrierファミリー22(SLC22)，有機アニオントランスポーター(OATP)についてmRNAの発現が確認されている[12)]。

このように，PXBマウス肝臓内のヒト肝細胞では，多数のヒト遺伝子およびタンパク質が発現して機能していることが確認されており，肝細胞を介する薬物代謝分野の研究において非常に有効なリソースであると考えられる。実際に，ヒトで利用されている医薬品に関連する研究として，Cefmetazole[17)]やWarfarin[18),19)]の体内動態(吸収，代謝，分布および排泄を含む)が，ヒト肝細胞の機能を反映していることが確認されている。また，ヒト臨床で薬物相互作用の1つとして問題となっている酵素誘導については，PXBマウスにRifampicinまたはRifabutinを反復投与した後にCYP3A4のmRNA発現量，タンパク質発現量およびタンパク質活性が増加することが確認されている[3),20)-22)]。これらの研究報告は，PXBマウスがヒト臨床での薬物相互作用の解析・研究において有用であることを示すデータと考えられる。

肝毒性研究分野では，医薬品や臨床試験段階にある化合物によって発生する肝障害が，ヒトの健康や製薬企業の医薬品開発に重大な影響を与えるため，PXBマウスを含む新しいリソースの登場によって，ヒトでの肝毒性発生を精度よく予測できることが期待されている。しかし，ヒト肝細胞キメラマウスには，肝毒性評価にあたって考慮すべき課題が3点挙げられる。1点目は，PXBマウスではuPA発現によってマウス肝細胞に障害が発生しているため，無処置でも血漿中ASTやALT測定値が高値を示し，またマウス肝細胞由来のASTとALTはヒト肝細胞に由来するこれら逸脱酵素と区別することが困難な点である(表2)。PXBマウスを利用してヒト肝細胞への毒性を検討する際には，これらマウス肝細胞由来の逸脱酵素の測定値のベースが高いことを踏まえ，被験物質の投与前後で同一個体での逸脱酵素の推移を確認することや組織観察によって肝障害の局在を確認することが必要と考えられる。2点目は，PXBマウスが免疫不全の形質を持つために，免疫系が関

表2　PXBマウスの血液生化学データ

項　目	単　位	平均 ±	標準偏差
GOT/AST	(U/l)	437.2 ±	504.8
GPT/ALT	(U/l)	280.3 ±	280.2
GGT	(U/l)	52.2 ±	24.0
CPK	(U/l)	275.4 ±	134.8
LDH	(U/l)	1165.9 ±	799.7
ALP	(U/l)	874.0 ±	421.1
LAP	(U/l)	86.6 ±	28.6
CHE	(U/l)	417.3 ±	82.4
AMYL	(U/l)	977.3 ±	363.3
BUN	(mg/dL)	35.6 ±	21.4
TCHO	(mg/dL)	135.3 ±	50.0
HDL-C	(mg/dL)	31.3 ±	15.2
TG	(mg/dL)	96.9 ±	37.3
TBIL	(mg/dL)	0.7 ±	0.4
DBIL	(mg/dL)	0.1 ±	0.0
GLU	(mg/dL)	118.3 ±	36.9
UA	(mg/dL)	3.5 ±	1.9
ALB	(g/dL)	2.7 ±	1.3
TP	(g/dL)	4.9 ±	0.4
CRE	(mg/dL)	255.6 ±	260.3
Ca	(mg/dL)	10.1 ±	1.2
IP	(mg/dL)	9.5 ±	1.6
Mg	(mg/dL)	2.6 ±	0.9

与する毒性の再現が困難な点，また3点目はPXBマウスの肝臓でヒト由来の成分は肝細胞のみであり，間質細胞はマウスに由来する点である。現在では，肝毒性発生の過程に免疫系や間質細胞が複雑に関与している可能性が示唆されているが，PXBマウスを用いてこのような肝毒性の全ての過程を再現することは困難である。現在，我々は業務提携先である積水メディカル㈱と共同して，PXBマウスを用いてヒト肝細胞を対象としたトキシコゲノミクスの構築を進めている。ヒト肝細胞での遺伝子発現の変化を基に，肝毒性発生を予想できるシステムとなることを期待したい。

肝炎ウイルス研究分野での利用は，PXBマウスの有効性が最も発揮されている例である。ヒト肝細胞キメラマウスが登場するまでは，チンパンジー以外に実用的なモデル動物が存在しなかった状況であったため，C型肝炎ウイルス(HCV)およびB型肝炎ウイルス(HBV)の2種類のウイルスに持続感染することが可能であり，またヒト臨床で使用されている代表的な治療薬の薬効が再現される点がPXBマウスの最大のアドバンテージとなっている。

HCVジェノタイプ1bを感染させて作製したHCV感染PXBマウスモデルを利用して，HCV治療薬であるPeg-IFNα-2aによる応答性を確認した試験の例を図7に示す。この試験では，HCV感染PXBマウスに，30μg/kgのPeg-IFNα-2aを1週間に2回の頻度で2週間反復皮下投与した後に2週間の休薬期間を設けた。その結果，Peg-IFNα-2aの投与によって血清中のHCV RNA濃度は速やかに減少し，投与終了後には血清中HCV RNA濃度の回復が確認された。HCV感染PXBマウスモデルを用いたHCV治療薬の評価に関しては，当社での検討の他にMyriocin(Serine palmitoyltransferase inhibitor)[23]，17-(dimethylaminoethylamino)-17-demethoxygeldanamycin(HSP90 inhibitor)[24]，DEBIO-025(Cyclophilin Inhibitor)[25]を検討した結果についても報告されている。

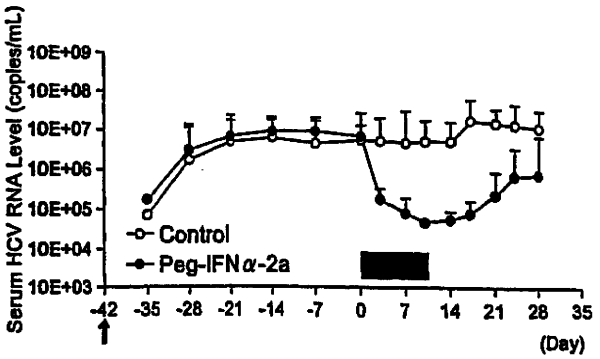

図7　HCV感染PXBマウスモデルでのPeg-IFNα-2a応答性

Peg-IFNα-2aにより血清中HCV RNA濃度が減少する。
矢印：HCV接種，灰色：Peg-IFNα-2a投与期間。

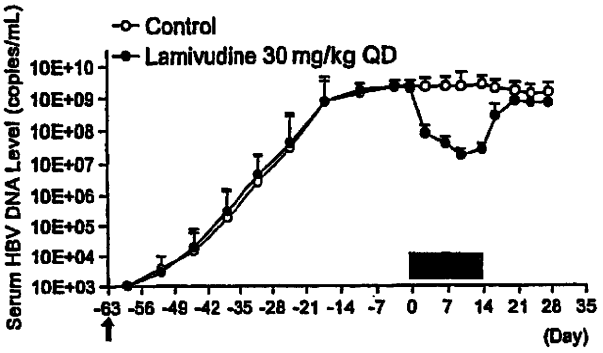

図8　HBV感染PXBマウスモデルでのLamivudine応答性

Lamivudineにより血清中HBV DNA濃度が減少する。
矢印：HBV接種，灰色：Lamivudine投与期間

HBVジェノタイプCを感染させて作製したHBV感染PXBマウスモデルを利用して，HBV治療薬であるLamivudineへの応答性を確認した試験の例を図8に示す。この試験では，Lamivudineの30 mg/kgを1日1回の頻度で2週間反復経口投与した後に2週間の休薬期間を設けた。その結果，Lamivudine投与によって血清中のHBV DNA濃度は緩やかに減少し，投与終了後は血清中HBV DNA濃度が速やかに回復した。HBV感染PXBマウスモデルに対するLamivudineの薬効に関しては，当社での検討の他に，Lamivudine耐性HBVを感染させたPXBマウスではLamivudineの抗HBV効果が減弱することが確認されている[26]。

5. おわりに

ヒト肝細胞研究のための新しいリソースとして，ヒト肝細胞キメラマウスは様々な研究分野で成果を上げている。今後，現状のuPA$^{+/+}$/SCIDマウスが抱えるいくつかの問題点，PXBマウスの用途上の制約を克服すべく研究開発を続けていきたいと考えている。

参考文献

1) Dandri M., Burda M. R., Török E., et al.: Repopulation of mouse liver with human hepatocytes and *in vivo* infection with hepatitis B virus. Hepatology, 33: 981–988, 2001.

2) Mercer D. F., Schiller D. E., Elliott J. F., et al.: Hepatitis C virus replication in mice with chimeric human livers. Nat. Med., 7: 927–933, 2001.

3) Tateno C., Yoshizane Y., Saito N., et al.: Near Completely Humanized Liver in Mice Shows Human-Type Metabolic Responses to Drugs. Am. J. Pathol., 165: 901–912, 2004.

4) Meuleman P., Libbrecht L., De Vos R., et al.: Morphological and Biochemical Characterization of a Human Liver in a uPA-SCID Mouse Chimera. Hepatology, 41: 847–856, 2005.

5) Morosan S., Hez-Deroubaix S., Lunel F., et al.: Liver-stage development of Plasmodium falciparum, in a humanized mouse model. J. Infect. Dis., 193: 996–1004, 2006.

6) Azuma H., Paulk N., Ranade A., et al.: Robust expansion of human hepatocytes in Fah$^{-/-}$/Rag2$^{-/-}$/Il2rg$^{-/-}$ mice. Nat. Biotechnol., 8: 903–910, 2007.

7) Suemizu H., Hasegawa M., Kawai K., et al.: Establishment of a humanized model of liver using NOD/Shi-scid IL2Rgnull mice. Biochem. Biophys. Res. Commun., 377: 248–252, 2008.

8) Heckel J. L., Sandgren E. P., Degen J. L., et al.: Neonatal Bleeding in Transgenic Mice Expressing Urokinase-Type Plasminogen Activator. Cell, 62: 447–456, 1990.

9) Sandgren E. P., Palmiter R. D., Heckel J. L., et al.: Complete Hepatic Regeneration after Somatic Deletion of an Albumin-Plasminogen Activator Transgene. Cell, 66: 245–256, 1991.

10) Kirchgessner C. U., Patil C. K., Evans J. W., et al.: DNA-dependent kinase (p350) as a candidate gene for the murine SCID defect. Science, 267: 1178–1183, 1995.

11) Kato M., Matsui T., Nakajima M., et al.: Expression of human cytochromes P450 in chimeric mice with human liver. Drug Metab. Dispos., 32: 1402–1410, 2004.

12) Nishimura M., Yoshitsugu H., Yokoi T., et al.: Evaluation of mRNA expression of human drug-metabolizing enzymes and transporters in chimeric mouse with humanized liver. Xenobiotica, 35: 877–890, 2005.

13) Uno S., Endo K., Ishida Y., et al.: CYP1A1 and CYP1A2 expression: comparing 'humanized' mouse lines and wild-type mice; comparing human and mouse hepatoma-derived cell lines. Toxicol. Appl. Pharmacol., 237: 119–126, 2009.

14) Kitamura S., Nitta K., Tayama Y., et al.: Aldehyde oxidase-catalyzed metabolism of N1-methylnicotinamide *in vivo* and *in vitro* in chimeric mice with humanized liver. Drug Metab. Dispos., 36: 1202–1205, 2008.

15) Katoh M., Sawada T., Soeno Y., et al.: *In vivo* drug metabolism model for human cytochrome P450 enzyme using chimeric mice with humanized liver. J. Pharm. Sci., 96: 428–437, 2007.

16) Katoh M., Matsui T., Okumura H., et al.: Expression of human phase II enzymes in chimeric mice with humanized liver. Drug Metab. Dispos., 33: 1333–1340, 2005.

17) Okumura H., Katoh M., Sawada T., et al.: Humanization of excretory pathway in chimeric mice with humanized liver. Toxicol. Sci., 97: 533–538, 2007.

18) Inoue T., Nitta K., Sugihara K., et al.: CYP2C9-Catalyzed Metabolism of S-Warfarin to 7-Hydroxywarfarin *in Vivo* and *in Vitro* in Chimeric Mice with Humanized Liver. Drug Metab. Dispos., 36: 2429–2433, 2008.

19) Inoue T., Sugihara K., Ohshita H., et al.: Prediction

of Human Disposition toward S-3H-Warfarin using Chimeric Mice with Humanized Liver. Drug Metab. Pharmacokinet., 24 : 153-160, 2009.

20) Katoh M., Matsui T., Nakajima M., et al. : *In vivo* induction of human cytochrome P450 enzymes expressed in chimeric mice with humanized liver. Drug Metab. Dispos., 33 : 754-763, 2005.

21) Katoh M., Watanabe M., Tabata T., et al. : *In vivo* induction of human cytochrome P450 3A4 by rifabutin in chimeric mice with humanized liver. Xenobiotica, 35 : 863-875, 2005.

22) Emoto C., Yamato Y., Sato Y., et al. : Non-invasive method to detect induction of CYP3A4 in chimeric mice with a humanized liver. Xenobiotica, 38 : 239-248, 2008.

23) Umehara T., Sudoh M., Yasui F., et al. : Serine palmitoyltransferase inhibitor suppresses HCV replication in a mouse model. Biochem. Biophys. Res. Commun., 346 : 67-73, 2006.

24) Nakagawa S., Umehara T., Matsuda C., et al. : Hsp90 inhibitors suppress HCV replication in replicon cells and humanized liver mice. Biochem. Biophys. Res. Commun., 353 : 882-888, 2007.

25) Inoue K., Umehara T., Ruegg U. T., et al. : Evaluation of a cyclophilin inhibitor in hepatitis C virus-infected chimeric mice *in vivo*. Hepatology, 45 : 921-928, 2007.

26) Yatsuji H., Noguchi C., Hiraga N., et al. : Emergence of a novel lamivudine-resistant hepatitis B virus variant with a substitution outside the YMDD motif. Antimicrob. Agents Chemother., 50 : 3867-3874, 2006.

(加国雅和／立野知世)

0090-9556/10/3811-1954–1961$20.00
DRUG METABOLISM AND DISPOSITION
Copyright © 2010 by The American Society for Pharmacology and Experimental Therapeutics
DMD 38:1954–1961, 2010

Vol. 38, No. 11
31732/3633215
Printed in U.S.A.

DMD

DRUG METABOLISM AND DISPOSITION

aspet

Effect of Hepatitis C Virus Infection on the mRNA Expression of Drug Transporters and Cytochrome P450 Enzymes in Chimeric Mice with Humanized Liver[S]

Ryota Kikuchi, Matthew McCown, Pamela Olson, Chise Tateno, Yoshio Morikawa, Yumiko Katoh, David L. Bourdet, Mario Monshouwer, and Adrian J. Fretland

Non Clinical Safety, Department of Drug Metabolism and Pharmacokinetics (R.K., D.L.B., M.Mo., A.J.F.), Viral Disease Biology Area (M.Mc.), and Molecular Medicine Laboratories (P.O.), Roche Palo Alto, Palo Alto, California; and PhoenixBio Co., Ltd., Higashi-Hiroshima, Japan (C.T., Y.M., Y.K.)

Received December 16, 2009; accepted August 6, 2010

ABSTRACT:

The expression of drug transporters and metabolizing enzymes is a primary determinant of drug disposition. Chimeric mice with humanized liver, including PXB mice, are an available model that is permissive to the in vivo infection of hepatitis C virus (HCV), thus being a promising tool for investigational studies in development of new antiviral molecules. To investigate the potential of HCV infection to alter the pharmacokinetics of small molecule antiviral therapeutic agents in PXB mice, we have comprehensively determined the mRNA expression profiles of human ATP-binding cassette (ABC) transporters, solute carrier (SLC) transporters, and cytochrome P450 (P450) enzymes in the livers of these mice under noninfected and HCV-infected conditions. Infection of PXB mice with HCV resulted in an increase in the mRNA expression levels of a series of interferon-stimulated genes in the liver. For the majority of genes involved in drug disposition, minor differences in the mRNA expression of ABC and SLC transporters as well as P450s between the noninfected and HCV-infected groups were observed. The exceptions were statistically significantly higher expression of multidrug resistance-associated protein 4 and organic anion-transporting polypeptide 2B1 and lower expression of organic cation transporter 1 and CYP2D6 in HCV-infected mice. Furthermore, the enzymatic activities of the major human P450s were, in general, comparable in the two experimental groups. These data suggest that the pharmacokinetic properties of small molecule antiviral therapies in HCV-infected PXB mice are likely to be similar to those in noninfected PXB mice. However, caution is needed in the translation of this relationship to HCV-infected patients as the PXB mouse model does not accurately reflect the pathology of patients with chronic HCV infection.

Introduction

Elimination of endogenous and exogenous substances is one of the most important physiological functions of the liver, which comprises the sinusoidal uptake from the blood circulation, intracellular phase I and phase II metabolism, and canalicular efflux of parent compound and/or metabolites into bile. Cumulative evidence suggests that members of the solute carrier (SLC) and ATP-binding cassette (ABC) transporters are expressed on either sinusoidal or canalicular membrane of the hepatocytes where they are responsible for the sinusoidal uptake and bile canalicular efflux of a diverse set of compounds (Chandra and Brouwer, 2004; Shitara et al., 2006; Dobson and Kell, 2008). On the other hand, cytochrome P450 enzymes are localized to the endoplasmic reticulum of hepatocytes and are the major enzymes involved in phase I drug metabolism and bioactivation, accounting for approximately 75% of the oxidative metabolism of marketed drugs (Gonzalez, 1990; Rendic and Di Carlo, 1997). Other enzymes such as glutathione transferase, UDP-glucuronosyltransferase, and sulfotransferase are involved in the conjugation of xenobiotics in phase II metabolism (Meyer, 1996; Williams et al., 2004). The expression and function of these transporters and enzymes are important determinants of the physiological turnover of endogenous compounds and clearance of exogenous substances including clinically used drugs.

Hepatitis C virus (HCV) infects an estimated 170 million people worldwide, and its infection is a leading cause of chronic hepatitis, liver cirrhosis, and hepatocellular carcinoma (World Health Organization, 1999). Currently, the combination therapy of pegylated interferon (IFN) and ribavirin is the only approved treatment for HCV infection. However, this treatment regimen is only effective in ap-

Article, publication date, and citation information can be found at http://dmd.aspetjournals.org.
doi:10.1124/dmd.109.031732.
[S] The online version of this article (available at http://dmd.aspetjournals.org) contains supplemental material.

ABBREVIATIONS: SLC, solute carrier; ABC, ATP-binding cassette; HCV, hepatitis C virus; IFN, interferon; uPA/SCID, urokinase plasminogen activator-transgenic severe combined immunodeficiency disorder; PCR, polymerase chain reaction; ISG, interferon-stimulated gene; hGAPDH, human glyceraldehyde-3-phosphate dehydrogenase; P450, cytochrome P450; LC, liquid chromatography; MS/MS, tandem mass spectrometry; MRP, multidrug resistance-associated protein; OATP, organic anion-transporting polypeptide; OCT, organic cation transporter; P-gp, P-glycoprotein; MDR, multidrug resistance; BSEP, bile salt export pump; NTCP, Na^+-taurocholate cotransporting polypeptide; OAT, organic ion transporter; C_t, cycle threshold.

proximately 50% of all patients infected with HCV. A number of individuals with HCV infection are unable to achieve a sustained virological response with the current therapy, and many of them will progress to liver diseases resulting from chronic infection with HCV. Thus, the development of more efficient therapies against HCV is of high priority (Wakita, 2007).

Several in vitro experimental models have been used to investigate the pathology of HCV as well as the efficacy of potential therapeutic compounds. These models include the use of individually cloned proteins of HCV (Littlejohn et al., 1998), infection of primary culture human hepatocytes with HCV (Buck, 2008), and in vitro HCV replicon systems in Huh-7 cells (Bartenschlager, 2005). The HCV replicon systems are particularly useful in HCV research and drug discovery because they are both permissive to high-efficiency HCV replication and respond to antiviral compounds including IFN-α and ribavirin. However, several limitations exist with the use of replicon systems in the discovery and development of novel anti-HCV compounds. These include the cell culture-adaptive mutations of the HCV genome and the innate difference of Huh-7 cells, which are immortalized tumor cells, compared with hepatocytes.

Because of the strict tropism of HCV, only humans and higher primates, such as chimpanzees, have, until recently, been receptive to authentic HCV infection and the development of chronic liver disease due to HCV infection (Lanford et al., 2001; Kremsdorf and Brezillon, 2007). However, use of chimpanzees is difficult from ethical and economical perspectives. The chimeric mouse with a humanized liver on the genetic background of urokinase plasminogen activator-transgenic severe combined immunodeficiency disorder (uPA/SCID) mice, designated as the PXB mouse, has been developed and characterized (Tateno et al., 2004). The livers of these mice are near completely (>70%) replaced with human hepatocytes and maintain the hepatic expression of most human drug-metabolizing enzymes and transporters (Nishimura et al., 2005). Subsequent studies have demonstrated that this mouse model is permissive to the infection of HCV in vivo and has potential utility in the discovery and development of new anti-HCV therapy (Umehara et al., 2006; Hiraga et al., 2007; Inoue et al., 2007). However, one should note that HCV-infected PXB mice do not precisely mimic chronic HCV infection in humans because these mice lack the adaptive immune response and liver disease associated with HCV infection as a result of their genetic background (SCID).

Because the primary organ of HCV infection and its replication is the liver, it is of great importance to know the possible alterations in the hepatic expression and activity of pharmacokinetics-related genes, i.e., drug transporters and metabolizing enzymes, by HCV infection. The aim of the present study was thus to investigate the effect of HCV infection on the mRNA expression of human ABC and SLC transporters and cytochrome P450 enzymes in the livers of PXB mice. Furthermore, the enzymatic activities of major human cytochrome P450 enzymes were compared between noninfected and HCV-infected PXB mice.

Materials and Methods

Generation of PXB Mice. PXB mice were generated by transplanting 1.0×10^6 human hepatocytes into the spleens of 2- to 3-week-old uPA/SCID mice under diethyl ether anesthesia as described previously (Tateno et al., 2004). All PXB mice used in the present study were derived from the same donor human hepatocyte (BD87, male, 2-year-old white; BD Biosciences, San Jose, CA).

Inoculation of HCV to PXB Mice. The inoculum used in the present study was HCV genotype 1b (HCR6, accession no. AY045702), which was obtained from HCV-infected PXB mice at the third passage. The original inoculum was obtained from the serum of an HCV-positive patient. PXB mice with a human albumin concentration in the blood greater than 6.0 mg/ml were infected with HCV genotype 1b at 9 to 10 weeks of age by injecting the inoculum (1.0×10^4 copies/mouse) to the retro-orbital sinus under diethyl ether anesthesia.

Quantification of Human Albumin Concentration and HCV Titer in the Serum. The concentration of human albumin in mouse blood was determined by latex agglutination immunonephelometry at 13 to 17 weeks of age. The replacement index is defined as the percentage of human hepatocyte repopulated in the host mouse liver and can be estimated from the blood human albumin value. RNA was extracted from the serum of PXB mice using a Sepa Gene RV-R RNA extraction system (Sanko Junyaku Co., Ltd., Ibaraki, Japan) according to the manufacturer's instructions, and the serum titer of HCV was determined by real-time quantitative PCR using TaqMan EZ RT-PCR Core Reagent and an ABI Prism 7500 sequence detector system as described previously (Takeuchi et al., 1999).

RNA Isolation and TaqMan Gene Expression Assays. Body weight was measured, and the liver was harvested from each mouse at 17 to 19 weeks of age. Total RNA was isolated from liver specimens using TRIzol (Invitrogen, Carlsbad, CA) according to the manufacturer's instructions and then treated with DNase I to remove contaminating genomic DNA. For cDNA synthesis, 80 ng of RNA was reverse-transcribed using a Transcriptor First Strand cDNA Synthesis Kit (Roche Applied Science, Indianapolis, IN) with random hexamer as the primer. The mRNA expression of human ABC transporters, SLC transporters, cytochrome P450 enzymes, and interferon-stimulated genes (ISGs) was quantified by TaqMan Gene Expression Assays on an ABI Prism 7900 system (Applied Biosystems, Foster City, CA) using LightCycler 480 Probe Master (Roche Applied Science) with primers and FAM-TAMRA or FAM-Iowa Black dual-labeled probes (Integrated DNA Technologies, Inc., Coralville, IA) that are specific for human genes. The protocol for PCR was as follows: 50°C for 2 min, 95°C for 10 min, and 40 cycles of 95°C for 15 s and 60°C for 1 min. The assay identification number or sequences of primers and probes used in the present study are listed in Table 1. The specificities of primers and probes to human genes were confirmed by comparing the amplification from human or mouse liver cDNA. No specific amplification was observed when mouse liver cDNA was used as a PCR template for all genes tested (data not shown). HCV RNA content in the livers of PXB mice was also quantified by TaqMan Gene Expression Assays using a cocktail of three forward primers, one reverse primer, and two TaqMan probes (Table 1) as described previously (Cook et al., 2004). The mRNA expression of each gene was quantified using the comparative C_t method, and normalized by the mRNA expression of hGAPDH.

Preparation of Liver Microsomes and Determination of Activities of Cytochrome P450 Enzymes. The microsomal fractions were isolated from the livers of noninfected and HCV-infected PXB mice at 18 or 20 weeks of age as described previously and stored at −70°C until further use (Sugihara et al., 2001). The activities of various P450s were determined in liver microsomes of PXB mice using selective substrates for the human P450 isoforms at appropriate concentrations (Table 2). In brief, 0.2 mg/ml microsomes were preincubated with substrate in 50 mM potassium phosphate buffer (pH 7.4) containing 5 mM $MgCl_2$ at 37°C for 5 min, and, subsequently, 2 mM NADPH was added to start the enzyme reaction. After the incubation at 37°C for 30 min (CYP1A2, CYP2C9, and CYP2C19), 15 min (CYP2D6), or 10 min (CYP3A4), the reaction was terminated by the addition of 150 μl of acetonitrile containing 7-hydroxycoumarin as an internal standard to 100 μl of incubation mixture. Samples were then centrifuged at 3000 rpm for 10 min at 4°C to precipitate the protein, and 10 μl of supernatant was analyzed by liquid chromatography (LC)-tandem mass spectrometry (MS/MS) to quantify the formation of metabolite. For the detection of acetaminophen, the supernatant as well as standard curves were further diluted with 5 mM ammonium acetate to ensure that the signal of each analyte was within the linear range of LC-MS/MS analysis. All of the experiments were conducted in triplicate.

LC-MS/MS Analysis. LC-MS/MS was performed on a Shimadzu high-performance liquid chromatography system with two LC-10ADvp pumps and the SCL-10Avp controller (Shimadzu Scientific Instruments, Columbia, MD) and an ABI Sciex API 4000 (Applied Biosystems). Samples were separated on a Hypersil BDS C18 column (50 × 2.1 mm, 5 μm; Thermo Fisher Scientific, Waltham, MA) with mobile phase A (0.1% formic acid in 5 mM ammonium acetate) and B (0.1% formic acid in acetonitrile/methanol 50/50, v/v) at a flow rate of 0.4 ml/min. High-performance liquid chromatography gradient programs were as follows: for CYP1A2, CYP2C9, and CYP2C19 assays,

TABLE 1

Assay identification number or sequences of primers and probes used for the TaqMan gene expression assays

Gene Name	RefSeq Identification	Assay Identification	Sequences (5′ to 3′)		
			Forward Primer	Reverse Primer	Probe
ABC transporters					
P-gp	NM_000927	Hs01067802_m1			
MDR3	NM_000443		CATCAATGACACCACTGAACTCAA	AACCTTGTCACCAATTCCTTCAC	CGCGGCTAACAGATGACATCTCCAAAA
BSEP	NM_003742		GGGCCATTGTACGAGATCCTAA	TGCACCGTCTTTTCACTTTCTG	TCTTGCTACTAGATGAAGCCACTTCTGCCTTAGA
MRP1	NM_004996		CATCGTGCAGGCGAGTGT	TCCTCACGGTGATGCTGTTC	TGACAGCATCGAGCGACGGCC
MRP2	NM_000392	Hs00166123_m1			
MRP3	NM_003786	Hs00358656_m1			
MRP4	NM_005845	Hs00195260_m1			
BCRP	NM_004827		CAGGTCTGTTGGTCAATCTCACA	TCCATATCGTGGAATGCTGAAG	CCATTGCATCTTGGCTGTCATGGCTT
SLC transporters					
NTCP	NM_003049		CCATGACACCACTCTTGATTGC	CGTCTGCACCGTCCATTG	ACCTCCTCCCTGATGCCTTTTATTGGC
OCT1	NM_003057	Hs00427550_m1			
OAT2	NM_006672		CTGCTAGTGTCCTCCGATATGAAG	GCACCGTAGGGTACAACTCTGAA	AAGCTGCCTTCACCACTGCCTACCTG
OATP1B1	NM_006446		GTACCACTTTCTTATTGCAACTCAGACT	CAGGGTGAGATGTAAGTTATTCCATTG	TCCACAGACTGGTTCCCATTGACTTTCA
OATP1B3	NM_019844	Hs00251986_m1			
OATP2B1	NM_007256		TCCTGTTTGCAGTGACCATGA	CACCTTCTGGCATCTGGTTAATG	CAGCCTCATGCTGCGCCTTTATGTG
Cytochrome P450 enzymes					
CYP1A1	NM_000499		TGGTCAAGGAGCACTACAAAACC	AGGTCCAAGACGATGTTAATGATCT	ATGAGAACGCCAATGTCCAGCTGTCA
CYP1A2	NM_000761		GGAGACCTTCCGACACTCCTC	CGTTGTGTCCCTTGTTGTGC	TTCTTGCCCTTCACCATCCCCAC
CYP2A6	NM_000762	Hs00711162_s1			
CYP2B6	NM_000767		TTGTTCTACCAGACTTTTTCACTCATC	GGAAAGTATTTCAAGAAGCCAGAGA	TCTGTATTCGGCCAGCTGTTTGAGCTC
CYP2C8	NM_000770	Hs00426387_m1			
CYP2C9	NM_000771	Hs00426397_m1			
CYP2C18	NM_000772	Hs00426403_m1			
CYP2C19	NM_000769	Hs00426380_m1			
CYP2D6	NM_000106	Hs00164385_m1			
CYP2E1	NM_000773	Hs00559368_m1			
CYP3A4	NM_017460		CAGGAGGAAATTGATGCAGTTTT	GTCAAGATACTCCATCTGTAGCACAGT	CCCAATAAGGCACCACCCACCTATGA
CYP3A5	NM_000777		TGGACTTTTTAAGAGACTGGGAATTC	AAATTTCCAGAGACCCTGACGAT	CACACCTCTGCCTTTGTTGGGAAATGTT
ISGs					
CIG5	NM_080657		AGATGTTTCTGAAGCGAGGA	GCAGACAATGGCAGTTACTC	TGGATTGGTAGAGCGGAAAGTGGA
G1P2	NM_005101		CTCATCTTTGCCAGTACAGG	AGCTCTGACACCGACAT	CCATGGGCTGGGACCTGACG
G1P3	NM_002038		AAGGCCCTGACCTTCAT	ATTCAGGATCGCAGACCA	AGGAGGACTCGCAGTCGCC
HSXIAPAF1	NM_017523		CTTGAGCACCAGCAGG	GCATGTCCAGTTTGCAGA	TCATAAGGCCAATGAGTGCCAGGA
IFI27	NM_005532		GTAGTTTTGCCCCTGGC	GACATCATCTTGGCTGCT	TGTGATTGGAGGAGTTGTGGCTGT
IFI35	NM_005533		CAAGATGAGGCTGTGGGA	AGACTTAGGCACTTCCGG	CCCCAAAGACAAGGTCCCATTTTCAG
IFI44	NM_006417		GCTACCCTCAGCTCTAGC	CGCTTCCCTCCAAAATGA	ACTGCCATACTTCTTGATCTGTTGTACTGT
IFIT2	NM_001547		AGGAAGATTTCTGAAGAGTGC	GTTCCAGGTGAAATGGCA	CACTGCAACCATGAGTGAGAACAATAAGAA
IFITM1	NM_003641		TCCTCATGACCATTGGATTCATC	CCGTTTTTCCTGTATTATCTGTAACATAA	AGACTGTCACAGAGCCGAATACCA
IRF7	NM_001572		GCAGCGTGAGGGTGTGTCTT	GGAAGCACTCGATGTCGTCAT	CCTGTCCAGCGCCAACAGCC
IRF9/ISGF3G	NM_006084	Hs00196051_m1			
MX1	NM_002462		AAGGAATGGGAATCAGTCATGAG	TCTATTAGAGTCAGATCCGGGACAT	CACCCTGGAGATCAGCTCCCGA
MX2	NM_002463		CTAGAGCTTCAGGACCCT	TGATGGTCAGGTCTGGAAC	CGTTCTGGGCTTTGTGTATCTCTTTCTC
OAS1	NM_016816		TGTGTGTCCAAGGTGGTAAAGG	CAACCAGGTCAGCGTCAGATC	CCTCAGGCAAGGGCACCACCCT
OAS2	NM_016817	Hs00942643_m1			
OAS3	NM_006187	Hs00196324_m1			
OASL	NM_003733	Hs00984390_m1			
SP110	NM_004510		CAAAGCGATGAGATCCTGAG	CTGAGTCTTCTTCCGCATTC	CTTGTCATTGGTCACTGAAGTGCTTCT
STAT1	NM_007315		GTGGAAAGACAGCCCTGCAT	ACTGGACCCCTGTCTTCAAGAC	AACGCACCCTCAGAGGCCGC
TLR3	NM_003265	Hs01551078_m1			
TNFSF10	NM_003810		TGCGTGCTGATCGTGATCTT	GTACTTGTCCTGCATCTGCTTCA	TGCTCCTGCAGTCTCTCTGTGTGGCT
TRIM22	NM_006074		GCAGGAGTTTGTGACCAA	AGAGGTTCTGTCAGGAGC	CCAAGGGAGCAGTGCAATGGATTT

TABLE 1—*Continued.*

Gene Name	RefSeq Identification	Assay Identification	Sequences (5' to 3')		
			Forward Primer	Reverse Primer	Probe
Others					
GAPDH	NM_002046		GAAGGTGAAGGTCGGAGTC	GAAGATGGTGATGGGATTTC	CAAGCTTCCCGTTCTCAGCC
HCV (5'-UTR)			GCGACACTCCACCATAGATCACT CGACACTCCACCATGAATCACT CACTCCGCCATGAAYCACT[a]	CACTCGCAAGCACCCTATCA	AGGCCTTTCGCGACCCAACACTACTC AGGCCTTTCGCAACCCAACGCTACT

UTR, untranslated region.
[a] Y = C or T.

1) mobile phase B was maintained at 5% for 1.0 min, 2) increased linearly to 90% from 1.0 to 2.0 min and maintained to 3.0 min, and 3) brought back to the initial concentration linearly from 3.0 to 3.1 min for reequilibration, total run time 4.0 min; for CYP2D6 assay, 1) mobile phase B was maintained at 5% for 1.0 min, 2) increased linearly to 95% from 1.0 to 2.0 min and maintained to 4.0 min, and 3) brought back to the initial concentration linearly from 4.0 to 4.1 min for reequilibration, total run time 6.0 min; and for CYP3A4 assay, 1) mobile phase B was maintained at 5% for 1.0 min, 2) increased linearly to 95% from 1.0 to 2.0 min and maintained to 3.0 min, and 3) brought back to the initial concentration linearly from 3.0 to 3.1 min for reequilibration, total run time 4.0 min. The MS/MS parameters and linear range of standard curves (limit of detection to maximum concentration) are listed for each metabolite in Table 2. Data were collected and processed using Sciex Analyst 1.4.2 data collection and integration software.

Statistical Analysis. Statistical analysis was performed by Student's *t* test using GraphPad Prism (version 4). Asterisks represent significant differences (*, $P < 0.05$, **, $P < 0.01$, and ***, $P < 0.001$, respectively) between noninfected and HCV-infected PXB mice.

Results

Human Albumin Concentration and HCV Titers in PXB Mice. Sex, human albumin concentration in the blood, body weight, serum HCV titers, and HCV RNA content in the liver are summarized in Table 3 for each mouse. The sex of PXB mice did not affect the activity of human cytochrome P450 enzymes derived from the human hepatocytes inside the host mouse liver (supplemental data). The average concentration of human albumin in the blood was not significantly different between noninfected and HCV-infected PXB mice. Accordingly, the replacement index of human hepatocytes estimated from the albumin concentration was similar between the two groups. Although body weight at the time of liver isolation was significantly higher in HCV-infected PXB mice than in noninfected mice for those used for the preparation of total liver RNA, the difference was not statistically significant in those used for the preparation of liver microsomes. Indeed, unpublished observations (C. Tateno) with different batches of HCV-infected mice suggested that HCV infection does not significantly affect the body weight of either male or female PXB mice. Serum HCV titers were determined in HCV-infected PXB mice, and HCV RNA content in the liver was measured in both noninfected and HCV-infected groups. A significant amount of HCV RNA was detected in both the serum and liver of HCV-infected mice, whereas HCV RNA was not detected in the liver of noninfected mice. These results confirmed that PXB mice were successfully infected by HCV.

Activation of Interferon-Signaling Pathways in HCV-Infected PXB Mice. Previous reports suggested that chronic infection with HCV is accompanied by the up-regulation of genes related to the interferon-signaling pathways in human patients (Smith et al., 2006). To corroborate the relevance of our experimental model in PXB mice to clinical HCV infection, the mRNA expression of human ISGs observed to be activated in HCV-infected patients was quantified in the livers of noninfected and HCV-infected mice. Fourteen of 22 ISGs investigated exhibited a significant increase in mRNA expression in the livers of HCV-infected PXB mice compared with that in noninfected mice (Fig. 1). The mRNA expression of MX2 was below the limit of detection in both groups. These results suggest that the interferon signaling pathways are activated by HCV infection in PXB mice, which is similar to what is observed in patients with chronic HCV infection.

mRNA Expression of Human ABC and SLC Transporters. The mRNA expression of major human hepatic ABC and SLC transporters was quantified in the livers of noninfected and HCV-infected PXB mice (Fig. 2). A significant increase in mRNA expression was ob-

TABLE 2

Substrate concentration and analytical parameters for each metabolite in MS/MS

Enzyme	Substrate	Metabolite	Mass Transition (m/z)	Mode	CE	DP	Linear Range
					eV	*eV*	
CYP1A2	Phenacetin (10 μM)	Acetaminophen	152.13 > 110.15	ESI+	22	46	10 nM–10 μM
CYP2C9	Diclofenac (5 μM)	4′-Hydroxydiclofenac	312.09 > 230.01	ESI+	45	41	1 nM–1 μM
CYP2C19	(*S*)-Mephenytoin (50 μM)	4′-Hydroxymephenytoin	235.10 > 150.21	ESI+	24	56	1 nM–1 μM
CYP2D6	Dextromethorphan (5 μM)	Dextrorphan	258.17 > 157.10	ESI+	51	81	1 nM–1 μM
CYP3A4	Midazolam (1 μM)	1′-Hydroxymidazolam	341.82 > 203.20	ESI+	38	71	1 nM–1 μM

CE, collision energy; DP, declustering potential; ESI, electrospray ionization.

TABLE 3

Human albumin concentration, estimated replacement index, body weight, and HCV content in the serum and liver of PXB mice

Animal	Sex	h-Alb	Estimated RI	Body Weight	Serum HCV Titer (10^7 copies/ml)	HCV RNA Content in the Liver (Relative to hGAPDH)
		mg/ml	%	*g*		
PXB mice used for the preparation of total liver RNA						
Noninfected						
PXB41-18	Male	6.3	74.2	14.4	—[a]	N.D.
PXB41-25	Male	8.2	82.3	13.7	—	N.D.
PXB42-1	Male	12.2	94.6	15.0	—	N.D.
Mean ± S.D.		8.9 ± 3.0	83.7 ± 10.3	14.3 ± 0.6	—	—
HCV-infected						
PXB36-11	Male	5.3	68.9	17.2	5.15	4.95×10^{-3}
PXB36-23	Male	7.7	80.4	16.8	5.52	3.53×10^{-3}
PXB38-11	Male	5.8	71.7	16.2	2.12	3.16×10^{-3}
Mean ± S.D.		6.3 ± 1.3	73.7 ± 6.0	16.7 ± 0.5*	4.26 ± 1.87	$3.88 \times 10^{-3} \pm 9.46 \times 10^{-4}$
PXB mice used for the preparation of liver microsomes						
Noninfected						
PXB22-47	Female	6.3	74.2	19.8	—	—
PXB22-48	Female	7.3	78.7	11.5	—	—
PXB22-57	Female	5.2	68.2	14.7	—	—
Mean ± S.D.		6.3 ± 1.1	73.7 ± 5.3	15.3 ± 4.2	—	—
HCV-infected						
PXB86-13	Male	6.3	74.2	22.8	6.56	—
PXB86-26	Female	3.5	55.9	19.4	0.806	—
PXB86-33	Male	6.4	74.6	22.1	4.66	—
Mean ± S.D.		5.4 ± 1.6	68.2 ± 10.7	21.4 ± 1.8	4.01 ± 2.93	—

h-Alb, human albumin; RI, replacement index; N.D., not detected.
* $P < 0.01$, significantly different between noninfected and HCV-infected PXB mice.
[a] —, not determined.

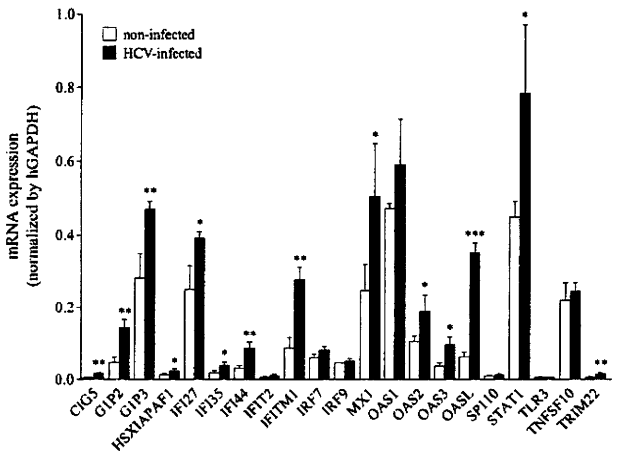

FIG. 1. Activation of interferon signaling pathways in HCV-infected PXB mice. The mRNA expression of human interferon-stimulated genes was measured in the livers of noninfected and HCV-infected PXB mice by TaqMan Gene Expression Assays as described under *Materials and Methods*, and the data were normalized by the mRNA expression of hGAPDH. Results are presented as the mean ± S.D. of three mice. □, mRNA expression in noninfected PXB mice; ■, mRNA expression in HCV-infected PXB mice. *, $P < 0.05$; **, $P < 0.01$; ***, $P < 0.001$, significantly different between noninfected and HCV-infected mice.

served for MRP4 and OATP2B1 in HCV-infected PXB mice compared with that in noninfected mice. In contrast, OCT1 was significantly decreased in HCV-infected PXB mice compared with that in their noninfected controls. The mRNA expression of MRP1 was below the limit of detection in both noninfected and HCV-infected groups. The mRNA levels of other ABC and SLC transporters, including P-gp, MDR3, BSEP, MRP2, MRP3, NTCP, OAT2, OATP1B1, and OATP1B3, were comparable between the two groups.

mRNA Expression of Human Cytochrome P450 Enzymes. The mRNA expression of 12 human cytochrome P450 genes, *CYP1A1*, *CYP1A2*, *CYP2A6*, *CYP2B6*, *CYP2C8*, *CYP2C9*, *CYP2C18*, *CYP2C19*, *CYP2D6*, *CYP2E1*, *CYP3A4*, and *CYP3A5*, was investigated in the livers of noninfected and HCV-infected PXB mice (Fig. 3). The mRNA expression of these genes was not statistically different between the two groups with the exception of significantly lower expression of CYP2D6 in HCV-infected mice.

Activity of Human Cytochrome P450 Enzymes. The activities of five major human cytochrome P450 enzymes, namely, CYP1A2, CYP2C9, CYP2C19, CYP2D6, and CYP3A4, were investigated in the liver microsomes of noninfected and HCV-infected PXB mice (Fig. 4). The metabolic activity in the liver microsomes from uPA/SCID mice for each probe substrate was comparable to or lower than that in human liver microsomes (C. Tateno, unpublished observations). Taking into account the fact that the livers of PXB mice are nearly completely (>70%) replaced with human hepatocytes, the background activity from remaining mouse hepatocyte in PXB

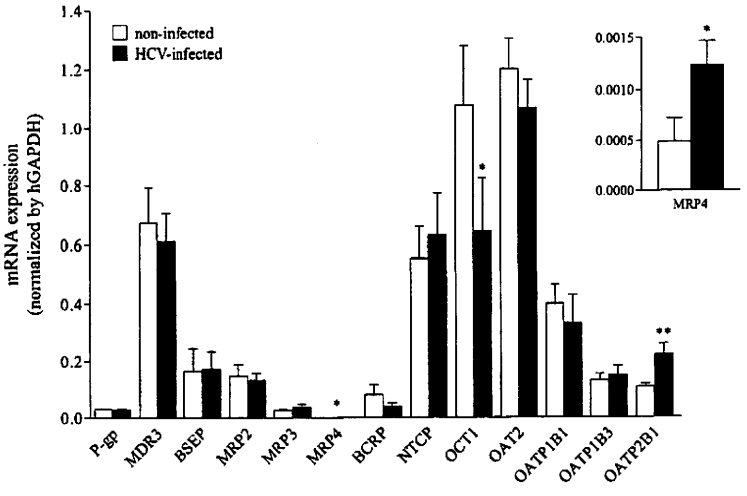

FIG. 2. mRNA expression profiles of drug transporters in PXB mice. The mRNA expression of human ABC and SLC transporters was measured in the livers of noninfected (□) and HCV-infected (■) PXB mice by TaqMan Gene Expression Assays, and the data are presented as described in the legend to Fig. 1. The inset represents the magnification of the mRNA expression of MRP4.

mice is minor. The metabolic activity of CYP1A2 was significantly lower in HCV-infected PXB mice than in noninfected PXB mice. The activities of other P450s were similar between noninfected and HCV-infected PXB mice.

Discussion

In the present study, the effect of HCV infection on the mRNA expression profiles of human ABC and SLC transporters and cytochrome P450 enzymes in PXB mice was investigated. The primers and probes specific for human genes were used in the TaqMan gene expression assays to exclude the background amplification of homologous genes from the host mouse liver. In addition, we have characterized enzymatic activities of major human P450s in the microsomes isolated from the livers of PXB mice.

The body weight and human albumin concentration in the blood of PXB mice were similar between noninfected and HCV-infected groups, suggesting that the inoculation of HCV does not affect the growth of transplanted human hepatocytes inside the host mouse liver or maturation of the mice (Table 3). A profound effect of HCV infection was observed on the status of interferon-signaling pathways, for which mRNA expression of a series of ISGs was significantly higher in the livers of HCV-infected PXB mice compared with that of noninfected controls (Fig. 1). The up-regulation of ISGs are in good agreement with the observation in patients with chronic HCV infection and chimpanzees with acute HCV infection (Su et al., 2002; Smith et al., 2006). In addition, these data are similar to the results published previously by Walters et al. (2006) who also used the human hepatocyte chimeric mouse model to examine the regulation of overall hepatic gene expression by HCV genotype 1a infection with microarray technology. It is of note that the effect of HCV infection on the expression of ISGs was comparable between genotype 1a (Walters et al., 2006) and 1b (this study). It is likely that there is no marked difference between the two HCV genotypes in terms of their effects on gene expression. It has been previously demonstrated that viremia in PXB mice can be reduced by treatment with IFN-α or pegylated-IFN as in human patients (Umehara et al., 2006; Hiraga et al., 2007; Inoue et al., 2007). The presence of functional interferon signaling pathways in PXB mice, suggested by the up-regulation of a number of ISGs by HCV infection, provides a rationale for the efficacy of those antiviral agents in this model. These observations warrant the use of PXB mice as an in vivo model for the primary infection of the liver by HCV to investigate the effects of novel anti-HCV compounds on suppressing the replication of HCV.

There were, in general, few marked differences in the mRNA expression of human ABC and SLC transporters and cytochrome P450 enzymes in the liver between noninfected and HCV-infected PXB mice with some exceptions, e.g., significantly higher expression

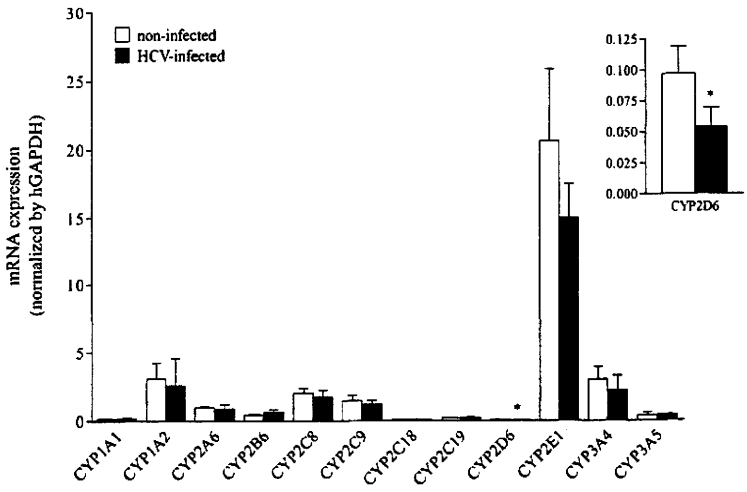

FIG. 3. mRNA expression profiles of drug-metabolizing enzymes in PXB mice. The mRNA expression of human cytochrome P450 enzymes was measured in the livers of noninfected (□) and HCV-infected (■) PXB mice by TaqMan Gene Expression Assays, and the data are presented as described in the legend to Fig. 1. The inset represents the magnification of the mRNA expression of CYP2D6.

DRUG METABOLISM AND DISPOSITION DMD aspet

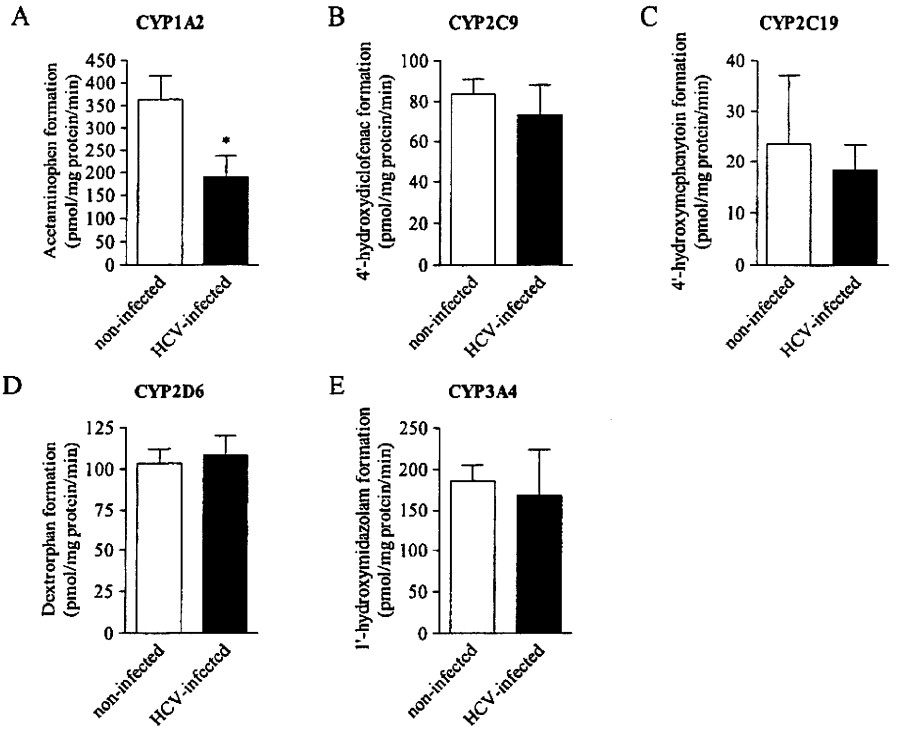

FIG. 4. Activity of human cytochrome P450 enzymes in PXB mice. The activities of five major human cytochrome P450 enzymes, i.e., CYP1A2 (A), CYP2C9 (B), CYP2C19 (C), CYP2D6 (D), and CYP3A4 (E), were measured in the liver microsomes of noninfected and HCV-infected PXB mice as described under *Materials and Methods*. Results are presented as the mean ± S.D. of three mice. □, metabolic activity in noninfected PXB mice; ■, metabolic activity in HCV-infected PXB mice. *, $P < 0.05$, significantly different between noninfected and HCV-infected mice.

of MRP4 and OATP2B1 and lower expression of OCT1 and CYP2D6 in HCV-infected mice than in noninfected mice (Figs. 2 and 3). Likewise, the activities of major human cytochrome P450 enzymes were similar between noninfected and HCV-infected PXB mice except for CYP1A2, which exhibited a significantly lower activity in HCV-infected PXB mice than in noninfected mice (Fig. 4). The effect of HCV infection on the mRNA expression and enzymatic activity of CYP1A2 and CYP2D6 was not consistent. The change in mRNA expression of CYP2D6 might not be sufficient to affect its enzymatic activity, whereas posttranscriptional effects of HCV infection may explain the decreased enzymatic activity of CYP1A2 regardless of unchanged mRNA expression. In consideration of the induction of many ISGs at the mRNA level, it is likely that the effect of HCV infection on the expression of pharmacokinetics-related genes would also be observed, if any, at the transcriptional level (CYP1A2 might be an exception). HCV infection probably affects gene expression via direct interference by virus infection, that is, the innate antiviral response and/or indirect interference by adaptive HCV-specific immune response, oxidative stress, and liver disease associated with chronic infection (Pawlotsky, 1998; Missale et al., 2004). PXB mice are immunocompromised because of their genetic background and thus lack the adaptive immune response and liver disease associated with HCV infection: i.e., there was no hepatocyte damage or inflammation in the liver of infected chimeric mice (Hiraga et al., 2007). HCV infection will thus affect gene expression only through the innate antiviral response in our experimental model. The similar expression profiles of drug transporters and metabolizing enzymes between noninfected and HCV-infected PXB mice suggest that innate antiviral signaling pathways play only a minor role in the regulation of mRNA expression of these genes.

There have been several reports regarding the aberrant mRNA expression of drug transporters and metabolizing enzymes in patients with HCV infection compared with those without infection or healthy volunteers. Hinoshita et al. (2001) have demonstrated that the mRNA expression of P-gp, MDR3, MRP1, MRP2, and MRP3 in the noncancerous region in the liver of patients with hepatic tumor tends to be lower in HCV-infected groups than in noninfected ones. On the other hand, Ros et al. (2003) have reported increased mRNA expression of P-gp and MRP3 in the livers of patients with HCV infection compared with healthy volunteers, whereas there was no significant difference for MRP2. Nakai et al. (2001) have performed a comprehensive study of variation in the mRNA levels of drug transporters and metabolizing enzymes in patients with chronic hepatitis C using quantitative real-time PCR and observed clear correlations between fibrosis stage and mRNA levels of CYP1A2, CYP2E1, CYP3A4, NTCP, OCT1, and OATP1B1 in the liver, whereas no fibrosis stage-dependent differences were observed for other transporters and enzymes that included P-gp, MDR3, MRP1, MRP2, and MRP3 (Nakai et al., 2008). Intriguingly, these clinical observations are inconsistent with the present findings in PXB mice in which HCV infection affects gene expression primarily through the innate antiviral response. The altered expression of drug transporters and metabolizing enzymes in clinical patients might be ascribed to the indirect interference by HCV infection or secondary effects as a result of the development of liver fibrosis or other hepatic dysfunction resulting from HCV infection. Indeed, serum levels or spontaneous productions by peripheral blood mononuclear cells of inflammatory cytokines such as tumor necrosis factor-α, interleukin-1β, and interleukin-6 were elevated in HCV-infected patients compared with those in healthy subjects (Kishihara et al., 1996; Huang et al., 1999; Cotler et al., 2001). In addition, several lines of evidence suggest perturbation of the expression of drug transporters and metabolizing enzymes by these cytokines both in vivo and in vitro (Lee and Piquette-Miller, 2003; Geier et al., 2005; Renton, 2005; Vee et al., 2009). Oxidative stress and liver diseases including cirrhosis and hepatocellular carcinoma, which are prevalent in patients with chronic HCV infection, also compromise the physiological expression of drug transporters (Bonin et al., 2002; Toyoda et al., 2008). This complex nature of HCV infection and progression to liver disease may

account for the controversial findings regarding the expression of pharmacokinetics-related genes in clinical patients with HCV infection, although the possibility of a difference in the patient population cannot be ruled out.

Because all PXB mice used in the present study are derived from a single donor hepatocyte, future studies are necessary to generalize the present findings by characterizing different batches of PXB mice originated from other donor hepatocytes. Nevertheless, the present study has clearly demonstrated that the infection of PXB mice, the chimeric mice with humanized liver, by HCV triggers the activation of interferon-signaling pathways as observed in human patients with chronic infection, but in general does not have a significant impact on the mRNA expression profiles of human ABC and SLC transporters or on the mRNA expression and enzymatic activity of cytochrome P450 enzymes. These results suggest that the pharmacokinetic behavior of small molecule antiviral therapies such as protease and polymerase inhibitors is likely to be comparable between HCV-infected and noninfected PXB mice. The PXB mouse model is a good model to study the effects of novel anti-HCV compounds in the primary treatment of HCV infection on suppressing the replication of HCV and therefore to investigate the relationship of the pharmacokinetics and pharmacodynamics of such therapies. However, caution is needed in the translation of this relationship to HCV-infected patients because PXB mice are immunocompromised based on their genetic background (SCID), and thus this mouse model does not accurately reflect the liver disease and immune response such as the increase in the levels of inflammatory cytokines observed in patients with chronic HCV infection, which may lead to changes in drug transporter and metabolizing enzyme expression.

Acknowledgments. We thank Drs. Yasuhisa Adachi and Shin-ichi Ninomiya for their technical assistance in the microsome assays.

References

Bartenschlager R (2005) The hepatitis C virus replicon system: from basic research to clinical application. *J Hepatol* **43**:210–216.

Bonin S, Pascolo L, Crocé LS, Stanta G, and Tiribelli C (2002) Gene expression of ABC proteins in hepatocellular carcinoma, perineoplastic tissue, and liver diseases. *Mol Med* **8**:318–325.

Buck M (2008) Direct infection and replication of naturally occurring hepatitis C virus genotypes 1, 2, 3 and 4 in normal human hepatocyte cultures. *PLoS One* **3**:e2660.

Chandra P and Brouwer KL (2004) The complexities of hepatic drug transport: current knowledge and emerging concepts. *Pharm Res* **21**:719–735.

Cook L, Ng KW, Bagabag A, Corey L, and Jerome KR (2004) Use of the MagNA pure LC automated nucleic acid extraction system followed by real-time reverse transcription-PCR for ultrasensitive quantitation of hepatitis C virus RNA. *J Clin Microbiol* **42**:4130–4136.

Cotler SJ, Reddy KR, McCone J, Wolfe DL, Liu A, Craft TR, Ferris MW, Conrad AJ, Albrecht J, Morrissey M, Ganger DR, Rosenblate H, Blatt LM, Jensen DM, and Taylor MW (2001) An analysis of acute changes in interleukin-6 levels after treatment of hepatitis C with consensus interferon. *J Interferon Cytokine Res* **21**:1011–1019.

Dobson PD and Kell DB (2008) Carrier-mediated cellular uptake of pharmaceutical drugs: an exception or the rule? *Nat Rev Drug Discov* **7**:205–220.

Geier A, Dietrich CG, Voigt S, Ananthanarayanan M, Lammert F, Schmitz A, Trauner M, Wasmuth HE, Boraschi D, Balasubramaniyan N, Suchy FJ, Matern S, and Gartung C (2005) Cytokine-dependent regulation of hepatic organic anion transporter gene transactivators in mouse liver. *Am J Physiol Gastrointest Liver Physiol* **289**:G831–G841.

Gonzalez FJ (1990) Molecular genetics of the P-450 superfamily. *Pharmacol Ther* **45**:1–38.

Hinoshita E, Taguchi K, Inokuchi A, Uchiumi T, Kinukawa N, Shimada M, Tsuneyoshi M, Sugimachi K, and Kuwano M (2001) Decreased expression of an ATP-binding cassette transporter, MRP2, in human livers with hepatitis C virus infection. *J Hepatol* **35**:765–773.

Hiraga N, Imamura M, Tsuge M, Noguchi C, Takahashi S, Iwao E, Fujimoto Y, Abe H, Mackawa T, Ochi H, Tateno C, Yoshizato K, Sakai A, Sakai Y, Honda M, Kaneko S, Wakita T, and Chayama K (2007) Infection of human hepatocyte chimeric mouse with genetically engineered hepatitis C virus and its susceptibility to interferon. *FEBS Lett* **581**:1983–1987.

Huang YS, Hwang SJ, Chan CY, Wu JC, Chao Y, Chang FY, and Lee SD (1999) Serum levels of cytokines in hepatitis C-related liver disease: a longitudinal study. *Zhonghua Yi Xue Za Zhi (Taipei)* **62**:327–333.

Inoue K, Umehara T, Ruegg UT, Yasui F, Watanabe T, Yasuda H, Dumont JM, Scalfaro P, Yoshiba M, and Kohara M (2007) Evaluation of a cyclophilin inhibitor in hepatitis C virus-infected chimeric mice in vivo. *Hepatology* **45**:921–928.

Kishihara Y, Hayashi J, Yoshimura E, Yamaji K, Nakashima K, and Kashiwagi S (1996) IL-1β and TNF-α produced by peripheral blood mononuclear cells before and during interferon therapy in patients with chronic hepatitis C. *Dig Dis Sci* **41**:315–321.

Kremsdorf D and Brezillon N (2007) New animal models for hepatitis C viral infection and pathogenesis studies. *World J Gastroenterol* **13**:2427–2435.

Lanford RE, Bigger C, Bassett S, and Klimpel G (2001) The chimpanzee model of hepatitis C virus infections. *ILAR J* **42**:117–126.

Lee G and Piquette-Miller M (2003) Cytokines alter the expression and activity of the multidrug resistance transporters in human hepatoma cell lines; analysis using RT-PCR and cDNA microarrays. *J Pharm Sci* **92**:2152–2163.

Littlejohn M, Locarnini S, and Bartholomeusz A (1998) Targets for inhibition of hepatitis C virus replication. *Antivir Ther* **3**:83–91.

Meyer UA (1996) Overview of enzymes of drug metabolism. *J Pharmacokinet Biopharm* **24**:449–459.

Missale G, Cariani E, and Ferrari C (2004) Role of viral and host factors in HCV persistence: which lesson for therapeutic and preventive strategies? *Dig Liver Dis* **36**:703–711.

Nakai K, Tanaka H, Hanada K, Ogata H, Suzuki F, Kumada H, Miyajima A, Ishida S, Sunouchi M, Habano W, Kamikawa Y, Kubota K, Kita J, Ozawa S, and Ohno Y (2008) Decreased expression of cytochromes P450 1A2, 2E1, and 3A4 and drug transporters Na^+-taurocholate-cotransporting polypeptide, organic cation transporter 1, and organic anion-transporting peptide-C correlates with the progression of liver fibrosis in chronic hepatitis C patients. *Drug Metab Dispos* **36**:1786–1793.

Nishimura M, Yoshitsugu H, Yokoi T, Tateno C, Kataoka M, Horie T, Yoshizato K, and Naito S (2005) Evaluation of mRNA expression of human drug-metabolizing enzymes and transporters in chimeric mouse with humanized liver. *Xenobiotica* **35**:877–890.

Pawlotsky JM (1998) Hepatitis C virus infection: virus/host interactions. *J Viral Hepat* **5(Suppl 1)**:3–8.

Rendic S and Di Carlo FJ (1997) Human cytochrome P450 enzymes: a status report summarizing their reactions, substrates, inducers, and inhibitors. *Drug Metab Rev* **29**:413–580.

Renton KW (2005) Regulation of drug metabolism and disposition during inflammation and infection. *Expert Opin Drug Metab Toxicol* **1**:629–640.

Ros JE, Libbrecht L, Geuken M, Jansen PL, and Roskams TA (2003) High expression of MDR1, MRP1, and MRP3 in the hepatic progenitor cell compartment and hepatocytes in severe human liver disease. *J Pathol* **200**:553–560.

Shitara Y, Horie T, and Sugiyama Y (2006) Transporters as a determinant of drug clearance and tissue distribution. *Eur J Pharm Sci* **27**:425–446.

Smith MW, Walters KA, Korth MJ, Fitzgibbon M, Proll S, Thompson JC, Yeh MM, Shuhart MC, Furlong JC, Cox PP, Thomas DL, Phillips JD, Kushner JP, Fausto N, Carithers RL Jr, and Katze MG (2006) Gene expression patterns that correlate with hepatitis C and early progression to fibrosis in liver transplant recipients. *Gastroenterology* **130**:179–187.

Su AI, Pezacki JP, Wodicka L, Brideau AD, Supekova L, Thimme R, Wieland S, Bukh J, Purcell RH, Schultz PG, and Chisari FV (2002) Genomic analysis of the host response to hepatitis C virus infection. *Proc Natl Acad Sci USA* **99**:15669–15674.

Sugihara K, Kitamura S, Yamada T, Ohta S, Yamashita K, Yasuda M, and Fujii-Kuriyama Y (2001) Aryl hydrocarbon receptor (AhR)-mediated induction of xanthine oxidase/xanthine dehydrogenase activity by 2,3,7,8-tetrachlorodibenzo-*p*-dioxin. *Biochem Biophys Res Commun* **281**:1093–1099.

Takeuchi T, Katsume A, Tanaka T, Abe A, Inoue K, Tsukiyama-Kohara K, Kawaguchi R, Tanaka S, and Kohara M (1999) Real-time detection system for quantification of hepatitis C virus genome. *Gastroenterology* **116**:636–642.

Tateno C, Yoshizane Y, Saito N, Kataoka M, Utoh R, Yamasaki C, Tachibana A, Soeno Y, Asahina K, Hino H, Asahara T, Yokoi T, Furukawa T, and Yoshizato K (2004) Near completely humanized liver in mice shows human-type metabolic responses to drugs. *Am J Pathol* **165**:901–912.

Toyoda Y, Hagiya Y, Adachi T, Hoshijima K, Kuo MT, and Ishikawa T (2008) MRP class of human ATP binding cassette (ABC) transporters: historical background and new research directions. *Xenobiotica* **38**:833–862.

Umehara T, Sudoh M, Yasui F, Matsuda C, Hayashi Y, Chayama K, and Kohara M (2006) Serine palmitoyltransferase inhibitor suppresses HCV replication in a mouse model. *Biochem Biophys Res Commun* **346**:67–73.

Vee ML, Lecureur V, Stieger B, and Fardel O (2009) Regulation of drug transporter expression in human hepatocytes exposed to the proinflammatory cytokines tumor necrosis factor-α or interleukin-6. *Drug Metab Dispos* **37**:685–693.

Wakita T (2007) HCV research and anti-HCV drug discovery: toward the next generation. *Adv Drug Deliv Rev* **59**:1196–1199.

Wakita T (2006) Host-specific response to HCV infection in the chimeric SCID-beige/Alb-uPA mouse model: role of the innate antiviral immune response. *PLoS Pathog* **2**:e59.

Williams JA, Hyland R, Jones BC, Smith DA, Hurst S, Goosen TC, Peterkin V, Koup JR, and Ball SE (2004) Drug-drug interactions for UDP-glucuronosyltransferase substrates: a pharmacokinetic explanation for typically observed low exposure (AUCi/AUC) ratios. *Drug Metab Dispos* **32**:1201–1208.

World Health Organization (1999) Global surveillance and control of hepatitis C. Report of a WHO Consultation organized in collaboration with the Viral Hepatitis Prevention Board, Antwerp, Belgium. *J Viral Hepat* **6**:35–47.

Address correspondence to: Dr. Adrian J. Fretland, Hoffmann-La Roche, 340 Kingsland St., Bldg. 123/1331, Nutley, NJ 07110-1199. E-mail: adrian.fretland@roche.com

Drug Metab. Pharmacokinet. 25 (6): 539-550 (2010).

Regular Article

In Vitro Evaluation of Cytochrome P450 and Glucuronidation Activities in Hepatocytes Isolated from Liver-Humanized Mice

Chihiro YAMASAKI[1,2], Miho KATAOKA[2], Yumiko KATO[1], Masakazu KAKUNI[1], Sadakazu USUDA[3], Yoshihiro OHZONE[4], Sunao MATSUDA[4], Yasuhisa ADACHI[4], Shin-ichi NINOMIYA[4], Toshiyuki ITAMOTO[5], Toshimasa ASAHARA[5], Katsutoshi YOSHIZATO[1,6] and Chise TATENO[1,2,*]

[1]*PhoenixBio, Co., Ltd., Higashihiroshima, Japan*
[2]*Cooperative Link of Unique Science and Technology for Economy Revitalization, Hiroshima Prefectural Institute of Industrial Science and Technology; Higashihiroshima, Japan*
[3]*ImmunoJapan Inc., Tokyo, Japan*
[4]*Sekisui Medical Inc., Tokai, Japan*
[5]*Hiroshima University, Graduate School of Biomedical Sciences, Division of Frontier Medical Science, Department of Surgery and Hiroshima University 21st Century COE Program for Advanced Radiation Casualty Medicine, Programs for Biomedical Research, Hiroshima, Japan*
[6]*Graduate School of Science, Hiroshima University, Higashihiroshima, Japan*

Full text of this paper is available at http://www.jstage.jst.go.jp/browse/dmpk

Summary: Cryopreserved human (h-) hepatocytes are currently regarded as the best *in vitro* model for predicting human intrinsic clearance of xenobiotics. Although fresh h-hepatocytes have greater plating efficiency on dishes and greater metabolic activities than cryopreserved cells, performing reproducible studies using fresh hepatocytes from the same donor and having an "on demand" supply of fresh hepatocytes are not possible. In this study, cryopreserved h-hepatocytes were transplanted into albumin enhancer/promoter-driven, urokinase-type plasminogen activator, transgenic/severe combined immunodeficient (uPA/SCID) mice to produce chimeric mice, the livers of which were largely replaced with h-hepatocytes. We determined whether the chimeric mouse could serve as a novel source of fresh h-hepatocytes for in vitro studies. h-Hepatocytes were isolated from chimeric mice (chimeric hepatocytes), and cytochrome P450 (P450) activities were determined. Compared with cryopreserved cells, the P450 (1A2, 2C9, 2C19, 2D6, 2E1, 3A) activities of fresh chimeric hepatocytes were similar or greater. Moreover, ketoprofen was more actively metabolized through glucuronide conjugates by fresh chimeric hepatocytes than by cryopreserved cells. We conclude that chimeric mice may be a useful tool for supplying fresh h-hepatocytes on demand that provide high and stable phase I enzyme and glucuronidation activities.

Keywords: human hepatocytes; chimeric mice; cytochrome P450; ketoprofen; UDP-glucuronosyltransferase

Introduction

"Chimeric mice" with livers repopulated with human hepatocytes (h-hepatocytes), created using urokinase-type plasminogen activator (uPA)/severe combined immunodeficient (SCID) mice,[1] were previously established and the expression of both cytochrome P450 enzymes (P450s, CYPs) and phase II enzymes in the liver of these chimeric mice, as well as *in vivo* induction of P450, were examined.[1-4]

P450 has been found to play an important role in the metabolism of xenobiotics, including drugs. Indeed, approximately 80% of oxidative metabolism is catalyzed by P450s,[5] and to predict pharmacokinetics and drug interactions precisely, investigation of the pharmacokinetics of a P450 substrate using chimeric mice would be of considerable value.

Species differences are known to exist in the metabolism of ketoprofen.[6] Ketoprofen is a propionic acid-class nonsteroidal anti-inflammatory drug with analgesic and

Received; May 17, 2010, Accepted; August 12, 2010, J-STAGE Advance Published Date; October 1, 2010
**To whom correspondence should be addressed:* Chise TATENO, Ph.D., *R&D Department, PhoenixBio, Co., Ltd., 3-4-1, Kagamiyama, Higashihiroshima, 739-0046, Japan. Tel/Fax. +81-82-431-0016, E-mail: chise.mukaidani@phoenixbio.co.jp*
This work was supported by CLUSTER and the Regional Science and Technology promotion budget.

antipyretic effects. Rat and mouse P450s primarily metabolize ketoprofen to hydroxyketoprofen.[6,7] In humans, ketoprofen is primarily metabolized by UDP-glucuronosyltransferase (UGT) and is converted to ketoprofen glucuronides.[8] Recently, it was demonstrated that when chimeric mice were administered ketoprofen, glucuronide conjugates were detected in their sera and bile. However, these conjugates are minor products; ketoprofen was primarily hydrolyzed in mice, and the main metabolites were hydrolyzed ketoprofen and glucuronide-conjugated ketoprofen.[7]

The metabolism of chemical entities has been examined using animals in the laboratory, but this approach fails to address differences in drug metabolism that exist between animal species. Because of the species differences in metabolic abilities, fresh h-hepatocytes are a better model for predicting the metabolism of drugs in the human body. For technical reasons, preparing fresh h-hepatocytes ahead of time and performing reproducible studies using the same donor are not possible. Thus, cryopreserved h-hepatocytes have been used, but they are compromised on thawing, resulting in decline and alteration of their normal function. Additionally, h-hepatocytes exhibit large individual differences in P450 activities. The differences might be due to real individual differences and/or the cryopreserving and thawing conditions.

We hypothesized that these practical problems in using h-hepatocytes for in vitro drug testing could be addressed if h-hepatocytes isolated from chimeric mouse livers exhibited human-type drug metabolism capacities in vitro. In the present study, we first determined the yield, viability, and purity of isolated h-hepatocytes from chimeric mice (chimeric hepatocytes). We compared the P450 activities of fresh and cryopreserved chimeric hepatocytes and assessed glucuronide activities toward ketoprofen using fresh and cryopreserved chimeric hepatocytes and cryopreserved donor hepatocytes.

We demonstrate that the chimeric mouse liver is a useful tool that can supply fresh hepatocytes retaining high P450 and UGT activities and allowing reproducible assays using hepatocytes derived from the same donor.

Materials and Methods

Materials: Phenacetin, tolbutamide, *S*-mephenytoin, dextromethorphan, chlorzoxazone, testosterone, ketoprofen, and Krebs-Henseleit buffer (KHB) were purchased from Sigma-Aldrich (St. Louis, MO). Coumarin and midazolam were obtained from Wako Pure Chemical Industries (Osaka, Japan). All other chemicals and solvents were of the highest or analytical grade commercially available.

Generation of mice with humanized livers: The present study was approved by the ethics committee of PhoenixBio Co., Ltd. and the Hiroshima Prefectural Institute of Industrial Science and Technology Ethics Board.

Cryopreserved h-hepatocytes from three donors (4YF, a 4-year-old Caucasian girl; 6YF, a 6-year-old African-American girl; and 2YM, a 2-year-old Caucasian boy) were purchased from BD Biosciences (San Jose, CA). Three (donor 4YF), 17 (donor 6YF), and 4 (donor 2YM) chimeric mice with humanized livers, generated by a method described previously, were used.[1] The concentration of human albumin (hAlb) in the blood of the chimeric mice and the replacement index (RI, the rate of hepatocyte replacement from mouse to human) were well correlated.[1] In the current study, we used 11–15-week-old male and female chimeric mice with approximately 11–14 mg/mL hAlb in mouse blood (RI > 70%); uPA/SCID mice were used as controls.

Isolation of hepatocytes from chimeric mouse liver, SCID mouse liver, and human liver tissue: Hepatocytes were isolated from the 4YF-, 6YF-, and 2YM-chimeric mice using a two-step collagenase perfusion method. The liver was perfused at 38°C for 10 min at 1.5 mL/min with Ca^{2+}-free and Mg^{2+}-free Hanks' balanced salt solution (CMF-HBSS) containing 200 mg/mL ethylene glycol tetraacetic acid (EGTA), 1 mg/mL glucose, 10 mM *N*-2-hydroxyethylpiperazine-*N'*-2-ethanesulfonic acid (HEPES), and 10 μg/mL gentamicin. The perfusion solution was then changed to CMF-HBSS containing 0.05% collagenase (Wako Pure Chemical Industries), 0.6 mg/mL $CaCl_2$, 10 mM HEPES, and 10 μg/mL gentamicin, and perfusion was continued for 17–23 min at 1.5 mL/min. The liver was dissected and transferred to a dish; liver cells were gently disaggregated in the dish with CMF-HBSS containing 10% bovine Alb, 10 mM HEPES, and 10 μg/mL gentamicin. The disaggregated cells were centrifuged three times (50 × *g*, 2 min). The pellet was suspended in medium consisting of Dulbecco's modified Eagle's medium (DMEM), 10% fetal bovine serum (FBS), 20 mM HEPES, 44 mM $NaHCO_3$, and antibiotics (100 IU/mL penicillin G and 100 μg/mL streptomycin). Cell number and viability were assessed using the trypan blue exclusion test.

Normal liver tissues were obtained from the resected liver of nine patients (51-, 53-, and 64-year-old men and a 68-year-old woman for plating efficiency; 54-, 57-, and 75-year-old men for P450 activity; and 55- and 69-year-old women for screening of monoclonal antibodies) after receiving consent prior to surgery, in accordance with the 1975 Declaration of Helsinki. Hepatocytes were isolated via two-step collagenase perfusion and low-speed centrifugation.[1] Aliquots of freshly isolated hepatocytes from four individuals, used for determining plating efficiency, were suspended at $1–2 \times 10^7$ cells/mL/vial in cryopreservation solution (Cellbanker; Juji Field, Inc., Tokyo, Japan), cryopreserved using a program freezer (Kryo-10 Series III; Planer Products Ltd., Sunbury-on-

Thames, Middlesex, UK), and kept in liquid nitrogen. To measure the plating efficiency of the hepatocytes, 4YF-chimeric hepatocytes and hepatocytes from human livers were inoculated onto 13.5-mm Celldesks (Sumitomo Bakelite, Tokyo, Japan) in 24-well plates (BD Biosciences) for 24 h, followed by fixation with ethanol and staining with hematoxylin and eosin. Adhered hepatocytes were counted under the microscope and plating efficiency was calculated by dividing number of adhered cells by the cell number inoculated in a well.

Hepatocytes were isolated from three male uPA (wt/wt)/SCID mice by collagenase perfusion methods.[9] They were used for *in vitro* glucuronidation activity studies.

Purification of h-hepatocytes from total hepatocytes of the chimeric mouse livers: A Fischer 344 rat was immunized intraperitoneally three times (once a week) with 10^7 mouse hepatocytes (m-hepatocytes) of SCID mice as an antigen, and injected with a booster of 2.5×10^7 m-hepatocytes at 3 weeks after the last immunization. Hybridomas were obtained by conventional methods and screened on immunohistochemical sections using m- and h- (from a 55-year-old woman) liver tissues. Frozen h- and m- liver sections were incubated with hybridoma supernatants and fluorescein-labeled anti-rat IgG antibodies (Alexa Fluor 594; Molecular Probes, Eugene, OR). Supernatants from 10 hybridoma clones were reacted with the plasma membrane of m-hepatocytes, but not with h-hepatocytes on the sections. The reactivity of each of the supernatants to the cell surface was determined with a fluorescence-activated cell sorter (FACS) as follows. Isolated m- and h- (69-year-old woman) hepatocytes were incubated with the supernatants and fluorescein isothiocyanate (FITC)-conjugated second antibodies (Alexa Fluor 488; Molecular Probes) and analyzed with a FACS Vantage SE (BD Biosciences) using a 100-μm nozzle. Fluorescence excited at 488 nm was measured through a 530-nm filter (FL1) with 4-decade logarithmic amplification. A hybridoma clone was selected as the clone that produced antibodies reactive to the cell surface of m-hepatocytes, but not h-hepatocytes. The antibody was purified from the culture medium of the hybridoma cells by protein G affinity column or ion exchange chromatography; the antibody was named 66Z.

Isolated h-hepatocytes from chimeric mice were contaminated with m-hepatocytes. To remove the m-hepatocytes, 6YF-hepatocytes isolated from the chimeric mice were incubated with the 66Z antibody, washed with DMEM containing 10% FBS, and incubated with Dynabeads M450-conjugated sheep anti-rat IgG (Dynal Biotech, Milwaukee, WI) in a tube for 30 min on ice. The tube was placed in Dynal MPC-1 (Dynal Biotech) for 1–2 min to remove 66Z-positive ($66Z^+$) m-hepatocytes. Enriched h-hepatocytes were collected as 66Z-negative ($66Z^-$) cells. Aliquots of chimeric hepatocytes from before and after enrichment were incubated with FITC-conjugated 66Z antibodies, and the proportion of $66Z^+$-cells in the h-hepatocytes was determined by FACS.

***In vitro* metabolic study using hepatocytes and microsomes:** For the measurement of the P450 activities of four fresh and five cryopreserved 6YF-chimeric mice, cryopreserved donor cells (6YF), and fresh h-hepatocytes from three individuals, suspended hepatocytes (6×10^4 cells) were incubated in KHB with each of eight substrates specific for seven P450 subtypes (phenacetin for CYP1A2, coumarin for CYP2A6, tolbutamide for CYP2C9, *S*-mephenytoin for CYP2C19, dextromethorphan for CYP2D6, chlorzoxazone for CYP2E1, and midazolam and testosterone for CYP3A) in 96-well plates (BD Biosciences) for 1 or 2 h (**Table 1**). The incubated solution was collected and an equivalent volume of methanol containing 1 μM niflumic acid (internal standard) was added. After centrifugation (10,000 rpm), the supernatant was subjected to liquid chromatography-tandem mass spectrometry (LC-MS/MS) (MDS SCIEX; Applied Biosystems, Foster City, CA). The LC system consisted of an HP 1100 system including a binary pump, an automatic sampler, and a column oven (Agilent Technologies, Waldbronn, Germany), equipped with a Symmetry Shield C18 column (Waters, Tokyo, Japan). The column temperature was 35°C. The mobile phase was 40% acetonitrile/0.1% formic acid (v/v). The flow rate was 0.3 mL/min. The LC was connected to a PE Sciex API2000 tandem mass spectrometer (Applied Biosystems), operated in positive electrospray ionization mode. The turbo gas was maintained at 550°C. Nitrogen was used as the nebulizing gas, turbo gas, and curtain gas at 65, 85, and 30 psi, respectively. Parent and/or fragment ions were filtered in the first quadrupole and dissociated in the collision cell using nitrogen as the collision gas. The analytical conditions for each substrate are shown in **Table 2**. The experiments were performed in triplicate per mouse, and the results are expressed as the average value of three mice or humans.

To assess changes in the P450 activities of fresh and cryopreserved 2YM-chimeric hepatocytes during storage at 4°C for 3 and 6 h, fresh and cryopreserved chimeric hepatocytes were prepared from two 2YM chimeric mice. The isolated hepatocytes from the chimeric mice were purified by isodensity centrifugation (27% Percoll, 7 min, 4°C) to remove dead hepatocytes. Cells (4×10^5 cells) were incubated in KHB with four different substrates specific for four P450s (phenacetin for CYP1A2, diclofenac for CYP2C9, *S*-mephenytoin for CYP2C19, and midazolam for CYP3A) in 24-well plates (BD Biosciences) for 2 h (**Table 1**). The incubated solution was collected and the concentration of the metabolites was measured by high-performance liquid chromatography (HPLC; Lachome Elite; Hitachi High-Technology Co., Tokyo, Japan). HPLC was performed at

Table 1. Reaction conditions for determination of CYP activities using cells and microsomes for LC-MS/MS and HPLC analysis

Enzymes measured	Enzyme activity	Substrate (concentration, mM)	Metabolite	Cells (LC-MS/MS)	Cells (HPLC)	Microsomes (LC-MS/MS)	
				Incubation time (h)	Incubation time (h)	Buffer*	Incubation time (min)
CYP1A2	Phenacetin *O*-deethylase	Phenacetin (15)	Acetaminophen	2	2	PB	20
CYP2A6	Coumarin 7-hydroxylase	Coumarin (8)	7-Hydroxycoumarin	2	–	TB	20
CYP2C9	Tolbutamide 4-hydroxylase	Tolbutamide (150)	Hydroxytolbutamide	2	–	TB	10
	Diclofenac 4′-hydroxylase	Diclofenac (100)	4-Hydroxydiclofenac	–	2	–	–
CYP2C19	*S*-Mephenytoin 4′-hydroxylase	*S*-Mephenytoin (20)	(±)-4′-Hydroxymephenytoin	2	2	PB	20
CYP2D6	Dextromethorphan *O*-demethylase	Dextromethorphan (8)	Dextrorphan	2	–	PB	20
CYP2E1	Chlorzoxazone 6-hydroxylase	Chlorzoxazone (100)	6-Hydroxychlorzoxazone	2	–	PB	20
CYP3A	Midazolam 1′-hydroxylase	Midazolam (10)	1′-Hydroxymidazolam	1	2	PB	10
	Testosterone 6β-hydroxylase	Testosterone (50)	6β-Hydroxytestosterone	2	–	PB	10

*TB, Tris-HCl buffer (pH 7.5); PB, potassium phosphate buffer (pH 7.4).

Table 2. Analytical parameters of LC-MS/MS for CYP1A2, 2A6, 2C9, 2C19, 2D6, 2E1, and 3A assays

Enzymes measured	Analyte	Mass spectrometer conditions						
		Mode	Declustering potential (eV)	Collision energy (eV)	Entrance potential (eV)	Collision cell exit potential (eV)	Ionspray voltage (V)	Analyte *m/z* transition
CYP1A2	Acetaminophen	Positive	40	25	7	10	5000	152.2→110.3
CYP2A6	7-Hydroxycoumarin	Positive	80	30	7	10	4200	162.8→107.2
CYP2C9	Hydroxytolbutamide	Positive	40	25	7	10	5000	286.9→171.3
CYP2C19	(±)-4′-Hydroxymephenytoin	Positive	80	25	7	10	4200	234.9→150.1
CYP2D6	Dextrorphan	Positive	120	40	7	10	4200	259.0→200.2
CYP2E1	6-Hydroxychlorzoxazone	Negative	−80	−25	−7	−10	−4200	184.1→120.0
CYP3A	6β-Hydroxytestosterone	Positive	60	25	7	10	4200	305.9→270.3
	1′-Hydroxymidazolam	Positive	100	40	7	10	5000	341.6→203.3
Ketoprofen	Ketoprofen	Positive	80	35	7	10	5000	255.5→104.9

a flow rate of 1.0 mL/min using the CAPCELL PAK C18, UG120 (4.6×250 mm, 5 μm; Shiseido, Tokyo, Japan) for CYP1A2 and CYP2C19, Inertsil ODS-3 (4.6×250 mm, 5 μm; GL Sciences Inc., Tokyo, Japan) for CYP2C9, and Xterra RP18 (4.6×150 mm, 5 μm; Waters) for CYP3A. Other analytical conditions are shown in **Table 3**. The measurements were performed in duplicate.

Liver microsomes were prepared from a 6YF-chimeric mouse and control uPA/SCID mice as described previously.[10] They were stored at −80°C until analysis. The protein concentration was determined using a Bradford protein assay kit (Bio-Rad, Hercules, CA), using bovine serum albumin as the standard. Microsomes from a chimeric mouse liver, pooled microsomes of six uPA/SCID mice, and pooled microsomes of 20 human livers (BD Gentest; BD Biosciences) were incubated with the substrates at 37°C for 5 min following incubation with the reduced form of nicotinamide adenine dinucleotide phosphate (NADPH) cofactor solution (3.8 mM β-$NADP^+$, 9.7 mM glucose-6-phosphate, 9.7 mM $MgCl_2$, 1.2 U/mL glucose-6-phosphate dehydrogenase) at 37°C for 10 or 20 min (**Table 1**). The incubated solution was collected and the concentration of the metabolites was measured by LC-MS/MS. The experiments were performed in triplicate per microsome preparation, and the results are expressed as the average value.

Detection of CYP2A6 gene mutations by the Invader assay: CYP2A6 polymorphism was determined by BML, Inc. (Tokyo, Japan). Genomic DNA was isolated from thawed human hepatocytes and the DNA was used

Table 3. Analytical conditions of HPLC for CYP1A2, 2C9, 2C19, and 3A assays

Enzymes measured	Analyte	Internal standard	Injection volume (μL)	Mobile phase				
				Solvent A*	Solvent B	Gradient program, %B (min)	Column temperature (°C)	UV detection (nm)
CYP1A2	Acetaminophen	0.1 μg Caffeine monohydrate	95	50 mM PB (pH 4.0)	Acetonitrile	Isocratic mode (A/B = 91/9)	35	245
CYP2C9	4′-Hydroxydiclofenac	0.4 μg Phenacetin	50	0.5% (v/v) AAAS	Methanol containing 0.5% (v/v) acetic acid	40 (0)→90 (30) →90 (35)→40 (36)	50	280
CYP2C19	(±)-4′-Hydroxymephenytoin	0.1 μg Phenobarbital sodium	95	50 mM PB	Acetonitrile	Isocratic mode (A/B = 80/20)	35	240
CYP3A	1′-Hydroxymidazolam	0.01 μg Phenacetin	50	10 mM PB (pH 7.4)	Acetonitrile/methanol mixture (7/5, v/v)	30 (0)→30 (5)→60 (17) →60 (25)→30 (26)	40	263

*PB, potassium phosphate buffer; AAAS, acetic acid aqueous solution.

for determining CYP2A6 polymorphism by the Invader assay.[11]

***In vitro* glucuronidation activity study using hepatocytes:** Ketoprofen metabolism was examined using three types of hepatocytes: fresh and cryopreserved 6YF-chimeric hepatocytes, cryopreserved donor cells (6YF), and fresh uPA(wt/wt)/SCID mouse hepatocytes. Hepatocytes (4×10^5 cells) suspended in KHB were plated in 24-well, non-treated plates (BD Biosciences) and incubated at 37 °C for 15 min. The cells were treated with 1 μM ketoprofen at 37 °C for 3 h. The medium was harvested and aliquots of the medium were incubated at 37 °C for 4 h with 0.25 M acetic acid buffer as a solvent control (A) and with 2500 units/mL β-glucuronidase (B). Equivalent 1 N KOH was added into (B) and incubated at 80 °C for 3 h (C). After incubation, an equivalent of methanol containing 1 μM niflumic acid (as an internal standard) was added. After centrifugation (10,000 rpm), the supernatant was subjected to LC-MS/MS.

The relevant concentrations can then be obtained:

[Concentration of ketoprofen in (B)] − [Concentration of ketoprofen in (A)] gives [Concentration of ketoprofen-glucuronide].

[Concentration of ketoprofen in (C)] − [Concentration of ketoprofen in (B)] gives [Concentration of transferred ketoprofen-glucuronide].

The transferred ketoprofen is the acyl glucuronide positional isomer, formed by acyl migration, which may be the glucuronide form transferred from ketoprofen-glucuronide during incubation. The experiments were performed in triplicate for a given mouse, and the results are expressed as the average value of three chimeric mice for fresh chimeric hepatocytes, the average of five chimeric mice for cryopreserved hepatocytes, and the average of three uPA(wt/wt)/SCID mice for fresh control mouse hepatocytes.

Statistics: The data were analyzed using Statcel2 (OMS Publishing Inc., Tokorozawa, Japan). Results are expressed as the mean ± SD, and the significance of the difference between two groups was analyzed by Student's *t*-test when data were normally distributed, and by Welch's *t*-test otherwise. $P < 0.05$ was deemed to indicate statistical significance.

Results

Yield, viability, and plating efficiency of isolated h-hepatocytes: Hepatocytes from the 4YF-, 6YF-, and 2YM-donors were transplanted into uPA/SCID mice, and chimeric mice were obtained bearing the respective donor hepatocytes (**Table 4**). The chimeric mice (4YF, 3 mice; 6YF, 17 mice; 2YM, 4 mice) were sacrificed at 54–83 days post-transplantation (**Table 4**). On the day they were sacrificed, blood was collected for the determination of hAlb concentrations (**Table 4**). Hepatocytes were then isolated by the collagenase perfusion method. Numbers (yield) of isolated viable hepatocytes were approximately $2–3 \times 10^7$ cells/mouse (**Table 4**). The viabilities were approximately 60–70% and 50–60% for fresh and cryopreserved chimeric hepatocytes, respectively, without Percoll purification.

The plating efficiency of hepatocytes from the chimeric mice was about 66.6 ± 3.4% (mean ± SD), while those of fresh hepatocytes and cryopreserved hepatocytes from human livers were 34.0 ± 19.3% and 9.3 ± 8.3%, respectively.

Purification of h-hepatocytes isolated from chimeric mice: Chimeric hepatocyte preparations consisted of h- and m-hepatocytes. It was found that 17.3 ± 6.7% of the fresh hepatocytes from 6YF-chimeric mice were $66Z^+$ ($n = 4$; **Table 4**) by FACS analysis. The enriched chimeric hepatocytes were found to be 3.3 ± 1.0% $66Z^+$ (m-hepatocytes; $n = 4$; **Table 4**).

P450 activities of hepatocytes from the chimeric mice: The P450 activities of hepatocytes from 6YF-chi-

Table 4. Hepatocytes used for the experiments

Purpose	Origin	Fresh or cryopreserved	n (sex of host animals or patients)	hAl in mouse blood (mg/mL)	Yield of hepatocytes ($\times 10^7$ cells)	Viability (%)	Ratio of mouse hepatocytes (%)	
							Before purification	After purification
Plating efficiency	Chimeric mouse (4YF)	Fresh	3 (M: 1, F: 2)	11.5±3.6	2.90±2.7/mouse	63.9±6.5	N.D.[*4]	N.D.
	Human liver (51–68-year-old)	Fresh	4 (M: 3, F: 1)	–	0.98±0.4/g liver	87.9±8.2	–	–
		Cryopreserved	4 (M: 3, F: 1)	–	–	56.2±7.5[*5]	–	–
CYP activities	Chimeric mouse (6YF)	Fresh	4[*1] (F)	11.8±0.6	1.78±0.9/mouse	61.8±6.9	17.3±6.7	3.3±1.0
		Cryopreserved	5[*2] (M: 2, F: 3)	12.6±2.1	–	60.5±10.6[*5]	5.8±4.7[*5]	2.1±1.0[*5]
	Human liver (54–75-year-old)	Fresh	3 (M: 3)	–	0.43±0.4/g liver	96.1±2.4	–	–
	Donor cell (6YF)	Cryopreserved	1 (F)	–	–	71.1	–	–
CYP activities at different time points after perfusion or thawing	Chimeric mouse (2YM)	Fresh	2[*3] (F)	11.8	3.05[*5,6]/mouse	84.8[*5,6]	N.D.	N.D.
		Cryopreserved	2[*3] (F)	11.8	–	86.4[*5,6]	N.D.	N.D.
Glucuronide activities	Chimeric mouse (6YF)	Fresh	3 (F)	13.5±2.9	3.24±1.0/mouse	69.8±11.2	9.8±2.0	–
		Cryopreserved	5 (M: 3, F: 2)	13.4±2.4	–	50.7±5.1[*5]	12.5±7.2	–
	Donor cell (6YF)	Cryopreserved	1 (F)	–	–	86.7	–	–
	uPA (wt/wt)/SCID mouse	Fresh	3	–	1.51±0.3/mouse	73.2±4.7	–	–

[*1] Hepatocytes from one of four mice were used for CYP1A2, 2C9, and 3A (testosterone), and those from another were used for CYP2A6, 2C19, 2D6, 2E1, and 3A (midazolam). Hepatocytes from two mice were used for all tested P450s.
[*2] Hepatocytes from one of five mice were used for CYP1A2, 2C9, and 3A (testosterone); those from a second mouse were used for CYP2A6, 2C19, and 2E1; those from a third mouse were used for CYP2C19, 2D6, 3A (midazolam); and those from a fourth mouse were used for tested P450s except for CYP2C19. Those from a fifth mouse were used for all tested P450s.
[*3] Hepatocytes from one of two mice were used for CYP1A2 and 3A, and those from the second mouse were used for CYP2C9 and 2C19.
[*4] Not determined.
[*5] Data after thaw.
[*6] Data after purification with Percoll.

meric mice were determined using eight substrates (**Table 1**). The reactions of P450 activities with all substrates shown in **Table 1** were linear with incubation time. The activities of fresh chimeric hepatocytes were compared with cryopreserved chimeric hepatocytes and cryopreserved donor cells. Three experiments were performed and the means±SD are given in **Figure 1**. CYP1A2, 2C19, and 2D6 activities in fresh chimeric hepatocytes were approximately twice those in cryopreserved cells (**Fig. 1**). CYP2A6, 2C9, 2E1, and 3A activities in fresh chimeric hepatocytes were similar to those of cryopreserved hepatocytes (**Fig. 1**). The activities of cryopreserved donor cells (6YF) were lower than those of cryopreserved 6YF-chimeric hepatocytes in CYP1A2, 2C19, and 3A (midazolam); higher in CYP2A6 and 2E1; and similar in CYP2C9, 2D6, 3A (testosterone; **Fig. 1**). Compared with CYP2A6 activities of two of the three fresh hepatocytes, CYP2A6 activity was extremely low in the chimeric hepatocytes (**Fig. 1**). Interestingly, the Invader assay revealed that donor 6YF had the *1/*4 CYP2A6 polymorphism; livers with the *1/*4 polymorphism in CYP2A6 are known to show low CYP2A6 activity.[12] We concluded that the low CYP2A6 activity was due to the *1/*4 polymorphism of donor 6YF. Three kinds of fresh h-hepatocytes were also examined for P450 activity. One of the three samples did not show CYP1A2 or 2C19 activity. Large individual differences were observed among the three in CYP2A6, 2C9, and 2E1 activities. The activities of CYP1A2, 2C19, 2D6, and 3A in fresh h-hepatocytes were lower than those in fresh chimeric hepatocytes.

We determined changes in the P450 activities of fresh and cryopreserved 2YM-chimeric hepatocytes after Percoll purification during storage at 4°C after isolation and thawing, respectively. CYP1A2, 2C9, 2C19, and 3A activities did not change for up to 6 h after isolation or thawing (**Fig. 2**). CYP1A2, 2C19, and 3A activities were lower in cryopreserved chimeric hepatocytes, and CYP2C9 activity was similar compared to fresh chimeric hepatocytes at 0 h after isolation or thawing (**Fig. 2**). The results were reproducible and are similar to those in **Figure 1**.

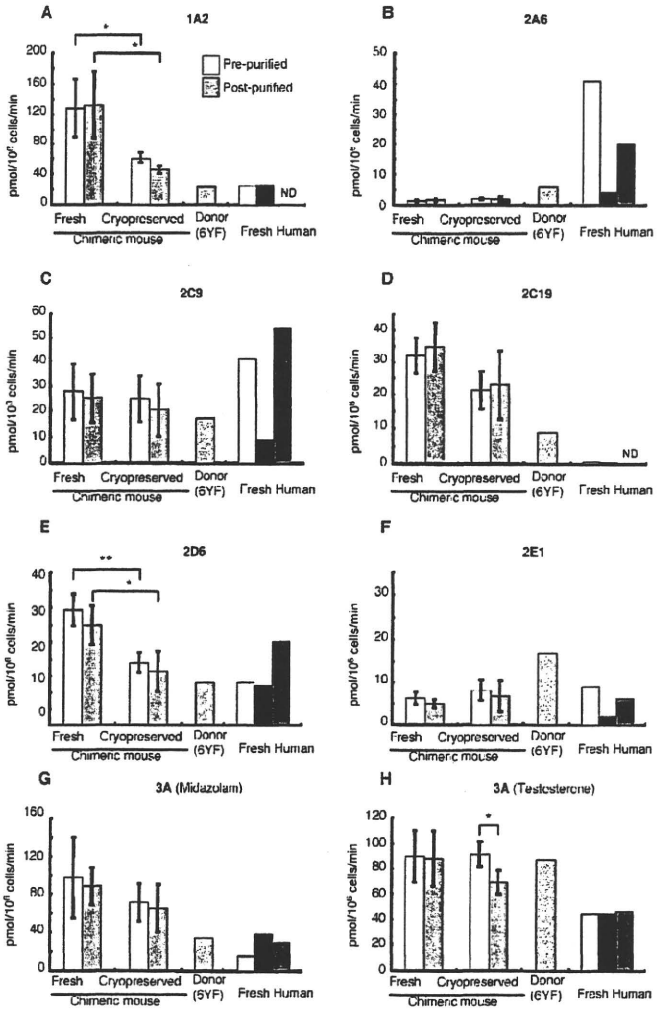

Fig. 1. P450 activities of fresh and cryopreserved chimeric hepatocytes, cryopreserved donor hepatocytes, and fresh h-hepatocytes, determined by LC-MS/MS

Hepatocytes were isolated from 6YF-chimeric mice. Aliquots of the isolated hepatocytes were frozen with a programmed freezer. Aliquots of fresh and thawed cryopreserved chimeric hepatocytes were purified with 66Z antibodies by magnetic sorting. Cryopreserved donor hepatocytes (6YF) for the chimeric mice were thawed. Fresh h-hepatocytes were isolated from resected livers after surgery from three patients. Eight kinds of suspended hepatocytes were incubated with eight substrates specific for seven P450s (**Table 1**): (A) 1A2, (B) 2A6, (C) 2C9, (D) 2C19, (E) 2D6, (F) 2E1, (G) 3A, midazolam, and (H) 3A, testosterone. The incubated medium was analyzed for each metabolite by LC-MS/MS (**Table 2**) and the metabolic activity of each P450 is shown as pmol/10^6 cells/min. Data in fresh and cryopreserved chimeric hepatocytes are shown as means ± SD of metabolite concentrations of three different chimeric mice. $^*p<0.05$, $^{**}p<0.01$. ND, not detected.

Contribution of m-hepatocyte contamination in chimeric hepatocytes to P450 activity: The proportions of m-hepatocytes in the fresh chimeric hepatocytes were approximately 17% and 3% before and after purification with 66Z antibodies, respectively, as described above. To determine how the contaminating m-hepatocytes affected P450 activities, we measured P450 activities using liver microsomes from a 6YF-chimeric mouse, pooled host uPA/SCID mice, and pooled human liver microsomes. Except for CYP2D6 and 2E1, P450 activities were similar or lower in uPA/SCID mouse liver microsomes than in human pooled microsomes (**Fig. 3**). Because the activities of CYP2D6 and 2E1 in uPA/SCID mouse liver microsomes were 50–100% higher than in pooled human microsomes (**Fig. 3**), we considered that m-hepatocytes contaminating the chimeric hepatocytes at around 17% might not significantly affect the activities of chimeric hepatocytes. We measured the P450 activity of pre- and post-purified chimeric hepatocytes (6YF) using 66Z antibodies. The purified hepato-